J. Fluid Mech. (2004), *vol.* 506, *pp.* 117–146.
DOI: 10.1017/S0022112004008560 Printed in the United Kingdom

Nonlinear stability of a visco-plastically lubricated viscous shear flow

By M. A. MOYERS-GONZALEZ[1], I. A. FRIGAARD[1,2]† AND C. NOUAR[3]

[1]Department of Mathematics, University of British Columbia, 1984 Mathematics Road, Vancouver, BC, V6T 1Z2, Canada

[2]Department of Mechanical Engineering, University of British Columbia, 2324 Main Mall, Vancouver, BC, V6T 1Z4, Canada

[3]LEMTA, CNRS UMR 7563, UHP & INPL, 2, Avenue de la foret de Haye, BP 160, 54504 Vandoeuvre, France

(Received 2 December 2002 and in revised form 14 November 2003)

A common problem in multi-layer shear flows, especially from the perspective of process engineering, is the occurrence of interfacial instabilities. Here we show how multi-layer duct flows can in fact be made nonlinearly stable, by using a suitable lubricating fluid. First we show how interfacial instabilities may be eliminated through the introduction of a yield stress fluid as the lubricant and by preserving an unyielded layer adjacent to the interface. Second we show how to treat the nonlinear stability of a two-layer flow, allowing finite motion of the domains. We focus on the simplest practically interesting case of visco-plastically lubricated viscous shear flow: a core–annular pipe flow consisting of a central core of Newtonian fluid surrounded by a Bingham fluid. We demonstrate that this flow can be nonlinearly stable at significant Reynolds numbers and produce stability bounds. Our analysis can be straightforwardly generalized to other flows in this class.

1. Introduction

A principal motivation for studying instabilities of multi-layer shear flows is their industrial relevance. Two broad application areas are the following.

(i) Co-extrusion processes: A co-extrusion operation essentially consists of combining several melt streams in a feedblock, from where the combined melt stream flows to the die and the layers take their final dimensions. Co-extrusion processes are extensively used in the production of bilayer and multi-layer films, sheets and pipes in the plastics industry, the concentric coating of two or more polymers and the production of conjugate fibres in the fibre industry. Interest in multi-layer extrusion has also grown due to its potential for producing composite products with improved material properties.

(ii) Lubricated pipelining: There is a tendency for two immiscible fluids to arrange themselves so that the low-viscosity constituent is in the region of high shear, i.e. typically closest to the wall in a duct flow. Thus, it appears possible to produce a beneficial effect in any flow of a very viscous liquid by introducing small amounts of a less viscous lubricating fluid. Such processes are used for example where a heavy

† Author to whom correspondence should be addressed.

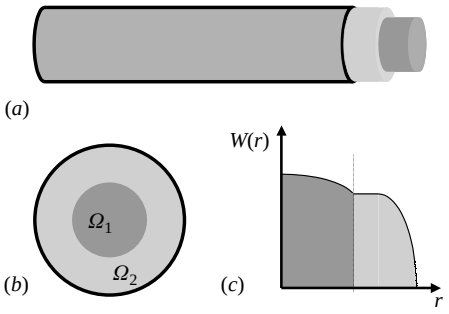

FIGURE 1. (*a*) A visco-plastically lubricated pipe flow. (*b*) Cross-section of the flow in the axisymmetric case, with Ω_1 (Newtonian fluid) lubricated by Ω_2 (Bingham fluid). (*c*) Schematic of the type of basic velocity profiles considered, with reduced rate of strain in the Newtonian fluid and an unyielded plug zone adjacent to the interface in the lubricating fluid.

crude oil is transported along pipelines with the addition of a small amount of water. Similar methods are used in coal–water slurry transport.

Particularly in co-extrusion operations, but also in other multi-layer flows, the rate of production (i.e. the flow rate), is limited by flow instabilities and especially by instabilities at the interfaces between adjacent layers. These instabilities can result in high scrap rates, in an economically infeasible process, or in final products with substandard mechanical, optical or barrier properties.

In this paper we focus on the stability of multi-layer duct flows in which the lubricating outer layer is a visco-plastic fluid and where both fluids are inelastic. Only iso-density fluids are considered. The basic flow we consider is a Poiseuille flow, driven by an axial pressure gradient with shear stress increasing in magnitude (linearly) from the channel centre outwards towards the walls. If we were to consider two Newtonian fluids in the configuration of figure 1(a,b), the flow would be linearly unstable at low Reynolds numbers. There have been many studies of such viscosity-stratified flows. The earliest is probably the classical study of Yih (1967). Later work includes studies of multi-layer Couette, Poiseuille and Couette–Poiseuille flows of Newtonian fluids, e.g. Hickox (1971), Hooper & Boyd (1987), Yiantsos & Higgins (1988). A fairly extensive review of this literature is given in Joseph & Renardy (1993), which also includes the many contributions of these authors to the study of lubricated pipelining flows. Broadly speaking, the linear stability of immiscible iso-density flows requires a sufficiently large surface tension and that the lubricating fluid be less viscous. Surface tension stabilizes short-wavelength interfacial modes and the viscosity ratio tends to stabilize long-wavelength instabilities.

Surprisingly, in this paper we establish nonlinear stability results for the configuration of figure 1(a,b), which are valid at moderate Reynolds numbers. For clarity we focus on a pipe flow in which the inner fluid is Newtonian and the outer fluid is Bingham, although our method of analysis is generally applicable a wide class of flows. The key to our results is as follows. A Bingham fluid behaves as a rigid solid in regions of the flow where the shear stress is below a critical *yield stress* value. Thus, since the shear stress increases linearly outwards in a duct flow, for a sufficiently large yield stress the Bingham fluid remains unyielded in a region that surrounds the inner fluid, see figure 1(*c*). The shear stress attains the yield stress only at the *yield surface*, which lies within the lubricating layer at some finite distance from the interface. The consequence of the above configuration is that, at the interface, the shear stress is below the yield stress by a finite amount. An infinitesimal (linear) perturbation

produces only an infinitesimal shear stress perturbation and hence is unable to break the unyielded region surrounding the interface. Thus, the key physical feature of lubricating with a yield stress fluid in the way described is that the interface cannot deform. Interfacial instabilities are therefore wholly eliminated. The above fact was first recognized in Frigaard (2001), where linear stability bounds were produced for visco-plastically lubricated multi-layer flows (of type similar to figure 1(*c*), and indeed critical Reynolds numbers were found to exceed those of the Newtonian problem. Here we consider nonlinear stability, which is clearly of interest for any practical flow situation.

In outline, our approach is as follows. First we consider only finite perturbations in which the magnitude of the shear stress perturbation is limited. This allows us to consider that unyielded Bingham fluid persists in a finite annular ring around the interface. Thus, again, the interface cannot deform. In such a situation, we are able to use energy stability methods. The approach follows that of e.g. Joseph (1976), with some adaptation for the yield stress, as developed by Nouar & Frigaard (2001). However, two cases must be considered: (i) that in which the central fluid region and surrounding plug does not translate within the cross-section of figure 1(*b*); (ii) where translational motion is possible.

Case (i) occurs when stress perturbations are close to being axisymmetric. This simpler case (see § 3) allows a clear exposition of the nonlinear stability method. We produce Reynolds number bounds for exponential decay of the L^2 norm of the perturbation. Case (ii) is clearly more challenging, and general (see § 4). We are again able to show exponential decay under conditions on the Reynolds number, but now the perturbation is not about the axisymmetric flow of figure 1, rather about a flow which is close to that in figure 1, but asymmetric (i.e. the central region in figure 1(*b*) can be translated a small finite amount). We obtain bounds for the departure from symmetry.

Apart from Newtonian fluids, a number of authors have considered the linear stability of multi-layer flows of other inelastic non-Newtonian fluids, e.g. power-law fluids are treated extensively in Waters (1983), Waters & Keeley (1987), Khomani (1990), Su & Khomani (1991), Carreau–Yasuda and Bingham-like fluids are treated in Pinarbasi & Liakopoulos (1995). In brief, these results are qualitatively similar to those found for Newtonian fluids, i.e. linear interfacial instabilities arise at small-to-moderate Reynolds numbers. Importantly, these studies do not consider fluids with a yield stress.† Explanations of the physical mechanisms that govern this type of instability for Newtonian fluids have been offered by Hinch (1984), Charru (1998), Charru & Hinch (2000), and we believe these explanations can be largely extended to purely viscous generalized Newtonian fluids. In simple terms, sufficiently close to the fluid–fluid interface, the non-Newtonian (nonlinear) character of any purely viscous generalized Newtonian fluid is simply not recognized, i.e. the dominant feature at the interface is a discontinuity in a finite constant viscosity between two fluids.

2. Model equations

In this paper we consider a multi-layer flow of two generalized Newtonian fluids along an infinite circular pipe. We focus on the case where the pipe cross-section is separated into two distinct fluid domains, with fluid 2 providing a lubricating layer for

† Pinarbasi & Liakopoulos (1995) do not consider a Bingham fluid with a yield stress, but instead they choose to regularize their rheological model, so that the effective viscosity attains a (large) Newtonian limit at zero shear rate. This modified constitutive model is then qualitatively similar to the Carreau–Yasuda model that is also studied in Pinarbasi & Liakopoulos (1995).

fluid 1, i.e. the cross-sectional domain occupied by fluid 1 is completely surrounded by fluid 2, which abuts the wall of the pipe, see figure 1. It will be assumed throughout that fluid 1 is a Newtonian fluid and fluid 2 is a Bingham fluid, although our analysis can be generalized without too much trouble to an arbitrary duct with an arbitrary generalized Newtonian fluid on the inside (fluid 1), lubricated by any generalized Newtonian fluid that has a yield stress, (fluid 2). For simplicity, we consider an arbitrary but finite length $\hat{L}$ of the pipe and later will consider nonlinear stability of the basic flows to perturbations that are $\hat{L}$-periodic with respect to the axial direction.

We denote the fluid domain by Ω and the two individual fluid domains by Ω_1 and Ω_2, respectively. The pipe and coordinates are aligned such that the $\hat{z}$-axis corresponds to the pipe axis. Fluid 1 has viscosity $\hat{\mu}^{[1]}$ and fluid 2 is characterized rheologically by its yield stress $\hat{\tau}^{[2]}_{yield}$ and plastic viscosity $\hat{\mu}^{[2]}$. It is assumed that both fluids have the same density $\hat{\rho}$ and surface tension is neglected. The total flow rate along the pipe is $\hat{Q}$ and the pipe radius is $\hat{R}$, thus defining the mean axial velocity: $\hat{U}_0 = \hat{Q}/\pi\hat{R}^2$. The pressure is denoted $\hat{p}(\hat{\boldsymbol{x}}, \hat{t})$, $\hat{\boldsymbol{u}}(\hat{\boldsymbol{x}}, \hat{t})$ is the velocity, $\hat{\tau_{ij}}^{[k]}$ denotes the deviatoric stress tensor in fluid k, and $\hat{g}_i$ is the gravitational acceleration in direction i.

The Navier–Stokes equations are made dimensionless with the following scaling:

$$\boldsymbol{x} = \frac{\hat{\boldsymbol{x}}}{\hat{R}}, \quad t = \frac{\hat{t}\hat{U}_0}{\hat{R}}, \quad \boldsymbol{u} = \frac{\hat{\boldsymbol{u}}}{\hat{U}_0}, \quad p = \frac{\hat{p}}{\hat{\rho}\hat{U}_0{}^2}, \quad \tau_{ij} = \frac{\hat{\tau}_{ij}\hat{R}}{\hat{\mu}^{[2]}\hat{U}_0}, \quad f_i = \frac{\hat{g}_i\hat{R}}{\hat{U}_0{}^2}, \tag{2.1}$$

leading to

$$\frac{\partial u_i}{\partial t} + u_j\frac{\partial u_i}{\partial x_j} = -\frac{\partial p}{\partial x_i} + \frac{1}{Re^{[2]}}\frac{\partial \tau_{ij}{}^{[k]}}{\partial x_j} + f_i, \quad k = 1, 2, \tag{2.2}$$

$$0 = \frac{\partial u_i}{\partial x_i}, \tag{2.3}$$

in each fluid domain. Constitutive laws for the two fluids are

$$\tau^{[1]}_{ij} = m\dot{\gamma}_{ij}, \tag{2.4}$$

$$\dot{\gamma}(\boldsymbol{u}) = 0 \Longleftrightarrow \tau^{[2]}(\boldsymbol{u}) \leqslant B, \tag{2.5}$$

$$\tau^{[2]}_{ij}(\boldsymbol{u}) = \left[1 + \frac{B}{\dot{\gamma}(\boldsymbol{u})}\right]\dot{\gamma}_{ij}(\boldsymbol{u}) \Longleftrightarrow \tau^{[2]}(\boldsymbol{u}) > B, \tag{2.6}$$

where

$$\dot{\gamma}_{ij} = \frac{\partial u_i}{\partial x_j} + \frac{\partial u_j}{\partial x_i},$$

$$\dot{\gamma}(\boldsymbol{u}) = \left[\frac{1}{2}\sum_{i,j=1}^{3}[\dot{\gamma}_{ij}(\boldsymbol{u})]^2\right]^{1/2}, \qquad \tau^{[2]}(\boldsymbol{u}) = \left[\frac{1}{2}\sum_{i,j=1}^{3}[\tau^{[2]}_{ij}(\boldsymbol{u})]^2\right]^{1/2}. \tag{2.7}$$

The three dimensionless parameters appearing above are defined by

$$m = \frac{\hat{\mu}^{[1]}}{\hat{\mu}^{[2]}}, \qquad Re^{[2]} = \frac{\hat{\rho}\hat{R}\hat{U}_0}{\hat{\mu}^{[2]}}, \qquad B = \frac{\hat{\tau}^{[2]}_{yield}\hat{R}}{\hat{U}_0\hat{\mu}^{[2]}}, \tag{2.8}$$

and are the viscosity ratio, fluid 2 Reynolds number and Bingham number, respectively. The fluid 1 Reynolds number $Re^{[1]}$ may be simply defined as $Re^{[1]} = mRe^{[2]}$. Boundary conditions are

$$\boldsymbol{u} = 0, \qquad x^2 + y^2 = 1, \tag{2.9}$$

$$\boldsymbol{u}(x, y, z, t) = \boldsymbol{u}(x, y, z + L, t). \tag{2.10}$$

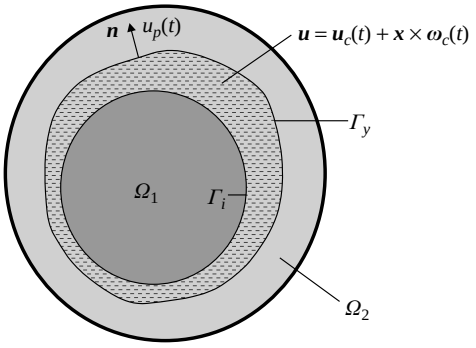

FIGURE 2. Schematic of the unyielded plug region.

2.1. *Interface and plug motion*

Across the interface (denoted Γ_i with unit normal $\boldsymbol{n}$), velocity and stress are continuous:

$$\boldsymbol{u} \text{ continuous on } \Gamma_i, \tag{2.11}$$

$$\left(-p\delta_{ij} + \frac{1}{Re^{[2]}}\tau_{ij}^{[k]}\right)n_j \text{ continuous on } \Gamma_i, \tag{2.12}$$

where δ_{ij} is the Kronecker delta.

To complete the classical formulation, (2.2)–(2.6), (2.9)–(2.12), we need consider how to determine the fluid motion within an unyielded region, say $\Omega_p(t) \subseteq \Omega_2(t)$. Although the momentum equations are satisfied in $\Omega_p(t)$, because (2.5) holds in such a *plug* region, the stresses are indeterminate. Kinematically, (2.5) implies that a plug moves as a rigid solid. However, a plug is not exactly a rigid solid, since mass may either enter or leave the plug through a yield surface. Determining the yield surfaces and their movement represent the key difficulties in dealing with visco-plastic fluid flows in a classical formulation.

For illustration and to pre-empt our later analysis, let us for the moment suppose that the domain Ω_1 is surrounded by an annular region $\Omega_p(t)$ of unyielded Bingham fluid. The plug is bounded by two surfaces: the interface Γ_i and an outer yield surface, say Γ_y, see figure 2. The outward normal to each surface is denoted by $\boldsymbol{n}$ and we suppose that the surfaces of the plug move instantaneously in the direction of $\boldsymbol{n}$ with speed u_p. The interface Γ_i is a material surface and consequently

$$u_p = u_j n_j, \qquad \boldsymbol{x} \in \Gamma_i, \tag{2.13}$$

which is effectively the kinematic equation for the interface motion. In contrast, the yield surface Γ_y is not a material surface. The speed of propagation of the yield surface in the normal direction, u_p, is determined wholly by changes in the deviatoric stress field, $\tau_{ij}^{[2]}$, which itself is fully determined only outside of the plug.

As with any rigid body motion, the velocity within the plug can be decomposed instantaneously into a linear motion and a rotation about a point. If we suppose (as we shall do later) that the annular plug region persists around $\Omega_1(t)$, then there can be no deformation of the interface and $\Omega_1(t)$ remains a uniform circular cylinder of radius r_i. We let $\boldsymbol{x}_c(t) = (x_c(t), y_c(t), z_c(t))$ denote a point on the axis of this cylinder, i.e. so that the interface position at time t is given by

$$r_i^2 = x_c^2(t) + y_c^2(t).$$

The plug velocity is then described instantaneously by the linear motion of the point $\boldsymbol{x}_c(t)$, which moves with velocity $\boldsymbol{u}_c(t)$, and by a rotation $\boldsymbol{\omega}_c(t)$ about $\boldsymbol{x}_c(t)$, i.e. $\boldsymbol{u} = \boldsymbol{u}_c(t) + (\boldsymbol{x} - \boldsymbol{x}_c) \wedge \boldsymbol{\omega}_c(t)$, or in component form

$$u_i = u_{c,i} + \epsilon_{ijk}(x_j - x_{c,j})\omega_{c,k},$$

where ϵ_{ijk} is the permutation symbol. The six unknowns: $u_{c,i},\ \omega_{c,i},\ i = 1, 2, 3$, must be determined from the six equations corresponding to conservation of linear and angular momentum. These equations are (for $i = 1, 2, 3$)

$$\begin{aligned} 0 = &\int_{\Omega_p(t)} (\dot{u}_{c,i} + \epsilon_{ijk}(x_j - x_{c,j})\dot{\omega}_{c,k})\,\mathrm{d}\boldsymbol{x} - \int_{\Gamma_y(t)} \sigma_{ij}^{[2]} n_j\,\mathrm{d}s - \int_{\Gamma_i(t)} \sigma_{ij}^{[1]} n_j\,\mathrm{d}s \\ &+ \int_{\Gamma_y(t)} (u_{c,i} + \epsilon_{ijk}(x_j - x_{c,j})\omega_{c,k})[(u_{c,l} + \epsilon_{lmn}(x_m - x_{c,m})\omega_{c,n})n_l - u_p]\,\mathrm{d}s \\ &- \int_{\Omega_p(t)} f_i\,\mathrm{d}\boldsymbol{x}, \end{aligned} \tag{2.14}$$

$$\begin{aligned} 0 = &\int_{\Omega_p(t)} \epsilon_{ijk}[x_j - x_{c,j}][\dot{u}_{c,k} + \epsilon_{klm}(x_l - x_{c,l})\dot{\omega}_{c,m}]\,\mathrm{d}\boldsymbol{x} - \int_{\Omega_p(t)} \epsilon_{ijk}(x_j - x_{c,j}) f_k\,\mathrm{d}\boldsymbol{x} \\ &- \int_{\Gamma_y(t)} \epsilon_{ijk}(x_j - x_{c,j})\sigma_{kl}^{[2]} n_l\,\mathrm{d}s - \int_{\Gamma_i(t)} \epsilon_{ijk}(x_j - x_{c,j})\sigma_{kl}^{[2]} n_l\,\mathrm{d}s \\ &+ \int_{\Gamma_y(t)} \epsilon_{ijk}[x_j - x_{c,j}][u_{c,k} + \epsilon_{klm}(x_l - x_{c,l})\omega_{c,m}] \\ &\times [(u_{c,l} + \epsilon_{lmn}(x_m - x_{c,m})\omega_{c,n})n_l - u_p]\,\mathrm{d}s. \end{aligned} \tag{2.15}$$

In (2.14) and (2.15) we have denoted the time derivatives of $u_{c,i},\ \omega_{c,i}$ by $\dot{u}_{c,i},\ \dot{\omega}_{c,i},\ i = 1, 2, 3$, and the stress tensors, $\sigma_{ij}^{[k]}$ are given by

$$\sigma_{ij}^{[k]} = -p\delta_{ij} + \frac{1}{Re^{[2]}}\tau_{ij}^{[k]}.$$

We have used continuity of the traction on Γ_i to replace $\sigma_{ij}^{[2]}$ with $\sigma_{ij}^{[1]}$. The surface integrals involving $\sigma_{ij}^{[k]}$ are understood to mean the limits of these integrals from the Newtonian fluid side and the yielded fluid region, i.e. from whichever side the stress is determinate.

The classical problem consists of (2.2)–(2.6) with (2.14) and (2.15), associated boundary conditions (2.2)–(2.6) and similar continuity conditions at the yield surface, i.e. the velocity and traction are continuous across a yield surface. Equations (2.14) and (2.15) constitute six nonlinear ordinary integro-differential equations† for $u_{c,i},\ \omega_{c,i},\ i = 1, 2, 3$, which are coupled to the flow outside the plug, through continuity of the traction and velocity vectors. This classical formulation is clearly extremely complex. To our knowledge, no solutions of such problems have been computed in multi-dimensions, without symmetry assumptions, even for a single fluid, and very little is known about the regularity of classical solutions to this problem. To avoid the inherent complexity of the classical formulation, it has been common to adopt a variational formulation, and to compute solutions using either regularization methods or an augmented Lagrangian approach.

† Note that since $x_{c,i},\ i = 1, 2, 3$ are obtained by integrating $u_{c,i},\ i = 1, 2, 3$, formally (2.14) and (2.15) are integro-differential equations.

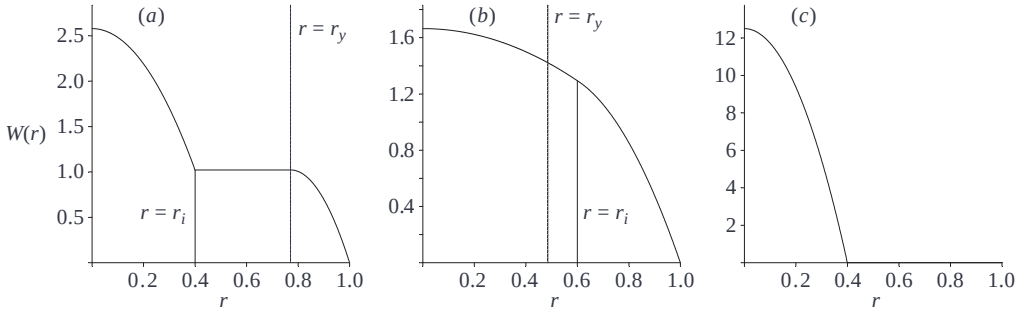

FIGURE 3. Examples of basic velocity profiles $W(r)$ illustrating the three different cases ($r = r_y$ and $r = r_i$ are marked with solid vertical lines): (*a*) case 1, $B = 30$, $r_i = 0.4$, $m = 2$; (*b*) case 2, $B = 5$, $r_i = 0.6$, $m = 5$; (*c*) case 3, $B = 50$, $r_i = 0.4$, $m = 0.3$ (here $r_y = 1.0666$).

3. Stationary Ω_1

In general, we consider conditional nonlinear stability, for which the finite stress perturbations are too weak to break the plug around Ω_1. Thus, the interface Γ_i does not deform and the shape of Ω_1 remains unchanged. In § 4 we shall allow Ω_1 to translate and rotate in the (x, y)-plane of figure 1(*b*). Since the pipe is assumed infinite and the perturbations are periodic in z, the above are the only kinematically possible motions of a non-deformed Ω_1. However, first we consider the simpler problem in which the domain Ω_1 does not move in the (x, y)-plane. For simplicity, we also impose that there is no perturbation of the plug region in the z-direction.

Since the interface is a material surface, the above restrictions are equivalent to demanding that $u_{c,i} = \omega_{c,i} = 0$, $i = 1, 2, 3$ are the solutions to (2.14) and (2.15), i.e. the plug region neither translates nor rotates. This is certainly true if we consider a linear perturbation of the axisymmetric basic steady flow of figure 1(*c*). This is because the normal modes, which would appear in boundary integrals of the linearized versions of (2.14) or (2.15), are integrated over an axial or azimuthal length, over which they vanish due to periodicity. An explicit example of this type is shown in detail in Frigaard, Howison & Sobey (1994), for a linear perturbation of plane Poiseuille flow. Thus, our assumption of stationary Ω_1 is satisfied by linear perturbations. For nonlinear perturbations, stationary Ω_1 results when there is zero net contribution to the moments exerted on the plug boundaries, which arises formally when axisymmetry of the stresses is assumed. This might be achieved for even a fully nonlinear perturbation, for example by the introduction of swirl into the flow, or by other means. Thus, our simplified problem is not wholly impractical.

3.1. *Basic flow*

The basic flow that we consider here is that in which a circular region of fluid 1 is surrounded concentrically by an annulus of fluid 2. In fact, three different types of basic flow can be found according to whether or not the Bingham fluid moves and whether or not the Bingham fluid is yielded at the interface. We illustrate the solution types in figure 3.

Assuming cylindrical coordinates (r, θ, z), the axisymmetric solution is $\boldsymbol{u} = (0, 0, W(r))$, with interface at $r = r_i$. We denote by $r = r_y$ the yield surface position, given by $r_y = 2B/G$, where $G = -Re^{[2]}\partial p/\partial z > 0$, and we have included the body force terms f_i into a modified pressure field.

Case 1: $r_y \in (r_i, 1)$, in which case there exists an unyielded plug surrounding the Newtonian region. This is the case of primary interest. The solution is given by

$$W(r) = \begin{cases} \dfrac{B}{2r_y}\left[\dfrac{1}{m}\left(r_i^2 - r^2\right) + (1-r_y)^2\right], & 0 \leqslant r \leqslant r_i, \\ \dfrac{B}{2r_y}(1-r_y)^2, & r_i < r \leqslant r_y, \\ \dfrac{B}{2r_y}[(1-r_y)^2 - (r-r_y)^2], & r_y < r \leqslant 1, \end{cases} \tag{3.1}$$

where $r_y \in (r_i, 1)$ is found as the root of the following quartic:

$$0 = (r_y)^4 - 4r_y\left(1 + \frac{3}{B}\right) + 3\left(1 + \frac{r_i^4}{m}\right), \tag{3.2}$$

which follows from a constraint on the flow rate, due to scaling with the mean velocity.

Case 2: $r_y \in [0, r_i)$, in which case the Bingham fluid region is entirely yielded. The solution is given by

$$W(r) = \begin{cases} \dfrac{B}{2r_y}\left[\dfrac{1}{m}\left(r_i^2 - r^2\right) + (1-r_y)^2 - (r_i - r_y)^2\right], & 0 \leqslant r \leqslant r_i, \\ \dfrac{B}{2r_y}[(1-r_y)^2 - (r-r_y)^2], & r_i < r \leqslant 1, \end{cases} \tag{3.3}$$

with r_y determined from

$$0 = r_y\left(4r_i^3 - 4 - \frac{12}{B}\right) + 3\left(1 + \frac{r_i^4}{m} - r_i^4\right). \tag{3.4}$$

Case 3: $r_y \in [1, \infty)$, in which case the Bingham fluid is wholly unyielded and does not flow. The solution is

$$W(r) = \begin{cases} \dfrac{B}{2r_y}\left[\dfrac{1}{m}\left(r_i^2 - r^2\right)\right], & 0 \leqslant r \leqslant r_i, \\ 0, & r_i < r \leqslant 1, \end{cases} \tag{3.5}$$

with r_y simply determined by

$$0 = 4r_y m - B r_i^4. \tag{3.6}$$

Solutions of this type, with a static wall layer, are the subject of ongoing investigation, see e.g. Allouche, Frigaard & Sona (2000), Frigaard, Leimgruber & Scherzer (2003), but are not of direct concern here.

In cases 2 and 3, the physical meaning of r_y is not as a yield surface, since r_y lies outside the Bingham fluid domain. The boundary of case 2 in the three-dimensional (r_i, B, m)-parameter space is where

$$B < \frac{12 r_i}{r_i^4(3/m + 1) - 4r_i + 3}. \tag{3.7}$$

The boundary of case 3 is where

$$B > \frac{4m}{r_i^4}. \tag{3.8}$$

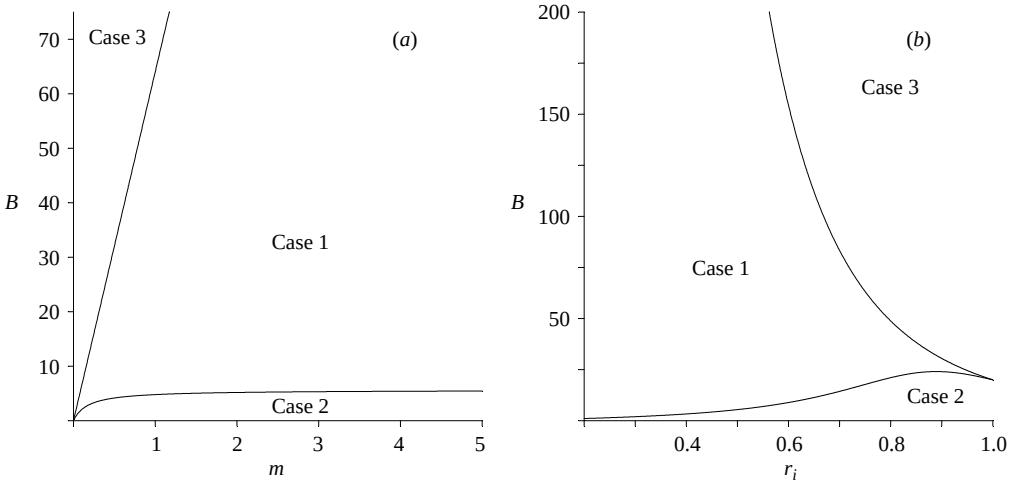

FIGURE 4. Parameter space in (r_i, B, m) for the three different basic solution types: (*a*) variations with B and m, for $r_i = 0.5$; (*b*) variations with B and r_i, for $m = 5$.

Figure 4 illustrates the dependence of the type of solution on the parameters r_i, B and m. Note from (3.7) that the boundaries between fully yielded and partially yielded cases satisfy the following asymptotic limits:

$$B \leqslant \frac{4m}{r_i^3} \quad \text{as } m \to 0, \tag{3.9}$$

$$B \leqslant \frac{12r_i}{r_i^4 - 4r_i + 3} \quad \text{as } m \to \infty, \tag{3.10}$$

$$B \leqslant 4r_i \quad \text{as } r_i \to 0, \tag{3.11}$$

$$B \leqslant \frac{4mr_i}{1 - 4(1 - r_i)} \quad \text{as } r_i \to 1. \tag{3.12}$$

Figure 4(*a*) shows typical variations with B and m, for fixed $r_i = 0.5$. Figure 4(*b*) shows typical variations with B and r_i for fixed $m = 5$. The primary focus of this paper is on the stability of basic solutions of type, case 1. It can be seen from figure 4 that such solutions are not hard to find in the (r_i, B, m)-parameter space.

3.2. *The Reynolds–Orr equation*

We consider nonlinear stability of (3.1) via the classical approach, using as a main tool the Reynolds–Orr equation, see e.g. Drazin & Reid (1981). The perturbed velocity and pressure fields are assumed periodic in the axial direction, and are denoted

$$\boldsymbol{U} + \boldsymbol{u} = (0, 0, W) + (u, v, w), \quad \boldsymbol{P} + \boldsymbol{p} = P + p,$$

where $W = W(r)$ is given by (3.1) and $P = P(z)$ is linear in z. The gradient of P is defined from r_y. We shall employ the notation (u_r, u_θ, w) to refer to the velocity field in cylindrical coordinates. Throughout, we make the following two assumptions:

(i) The Newtonian domain Ω_1 remains stationary (see the earlier discussion).

(ii) The deviatoric stress of the nonlinear perturbation satisfies a bound of form

$$\left|{\tau_{ij}}^{[k]}(\boldsymbol{U} + \boldsymbol{u}) - {\tau_{ij}}^{[k]}(\boldsymbol{U})\right| < a, \quad k = 1, 2;\ i, j = 1, 2, 3, \tag{3.13}$$

for some $a > 0$. The choice of a sufficiently small (but finite) bound a is made, so that we are able to ensure that the perturbed flow retains an unyielded plug region about

Ω_1. To see that this is feasible, note that the unperturbed stress varies linearly with r:

$$\tau^{[2]}(\boldsymbol{U})(r) = \left|\tau_{rz}{}^{[2]}(\boldsymbol{U})\right|(r) = \frac{r}{r_y}B.$$

Thus, from (3.13) we see that

$$\tau^{[2]}(\boldsymbol{U}+\boldsymbol{u}) \leqslant \left[\left(a+\frac{r}{r_y}B\right)^2 + \frac{7}{2}a^2\right]^{1/2},$$

and for $r \in (r_i, r_y)$ the perturbed flow is unyielded in (r_i, r) provided that

$$a < a_{\max}(r_i, B, m) = \frac{2B}{9}\left(\left[\frac{9}{2} - \frac{7}{2}\left(\frac{r}{r_y}\right)^2\right]^{1/2} - \frac{r}{r_y}\right). \tag{3.14}$$

We will relax the first of the above assumptions in § 4, but we will retain a form of the second assumption. This second assumption is used in stability problems involving yield stress fluids and its purpose is to ensure that a region of unyielded fluid persists under the action of the perturbation. For linear stability, a becomes infinitesimal and (3.13) has the physical implication that a finite plug region is not destroyed by an infinitesimal perturbation, which allows one to consider a linear perturbation of the yield surface; see e.g. Frigaard *et al.* (1994), Frigaard (2001). For nonlinear stability, (3.13) makes the stability bounds conditional, but these are not necessarily weakly nonlinear perturbations; see e.g. Nouar & Frigaard (2001).

The equations of motion in each (now fixed) domain, $\Omega_k : k = 1, 2$, are

$$0 = -\frac{\partial P}{\partial x_i} + \frac{1}{Re^{[2]}}\frac{\partial}{\partial x_j}\tau_{ij}{}^{[k]}(\boldsymbol{U}), \tag{3.15}$$

$$0 = \frac{\partial U_i}{\partial x_i}, \tag{3.16}$$

$$\left[\frac{\partial}{\partial t} + (U_j + u_j)\frac{\partial}{\partial x_j}\right](U_i + u_i) = -\frac{\partial}{\partial x_i}(P+p) + \frac{1}{Re^{[2]}}\frac{\partial}{\partial x_j}\tau_{ij}{}^{[k]}(\boldsymbol{U}+\boldsymbol{u}), \tag{3.17}$$

$$0 = \frac{\partial}{\partial x_i}(U_i + u_i). \tag{3.18}$$

Note that $U_j \partial U_i/\partial x_j = 0$. We subtract (3.15) from (3.17), multiply by u_i, and integrate over the individual fluid domains to give

$$\int_{\Omega_k} u_i \frac{\mathrm{D}}{\mathrm{D}t}u_i \,\mathrm{d}\boldsymbol{x} = -\int_{\Omega_k}\left[u_j\frac{\partial W}{\partial x_j}\right]w\,\mathrm{d}\boldsymbol{x} - \frac{1}{Re^{[2]}}\int_{\Omega_k}\frac{\partial u_i}{\partial x_j}\left[\tau_{ij}{}^{[k]}(\boldsymbol{U}+\boldsymbol{u}) - \tau_{ij}{}^{[k]}(\boldsymbol{U})\right]\mathrm{d}\boldsymbol{x}$$
$$+ \int_{\partial\Omega_k} u_i\left[-p + \frac{1}{Re^{[2]}}\left[\tau_{ij}^{[k]}(\boldsymbol{U}+\boldsymbol{u}) - \tau_{ij}^{[k]}(\boldsymbol{U})\right]\right]n_i^{[k]}\,\mathrm{d}s, \tag{3.19}$$

where we have used the divergence theorem to derive the last term, $\boldsymbol{n}^{[k]}$, denoting the outward normal to the boundary $\partial\Omega_k$ of Ω_k. We now sum the two fluid domains in (3.19). Note that all the boundary integrals vanish, through a combination of: (i) boundary conditions at the wall, (ii) periodicity at the ends of the domain considered, (iii) continuity of velocity and traction vectors at the interface. Thus, finally we have

$$\frac{\mathrm{d}}{\mathrm{d}t}\sum_k\int_{\Omega_k}\frac{u_i^2}{2}\,\mathrm{d}\boldsymbol{x} = -\sum_k\int_{\Omega_k}u_r\frac{\partial W}{\partial r}w + \frac{1}{Re^{[2]}}\frac{\partial u_i}{\partial x_j}\left[\tau_{ij}{}^{[k]}(\boldsymbol{U}+\boldsymbol{u}) - \tau_{ij}{}^{[k]}(\boldsymbol{U})\right]\mathrm{d}\boldsymbol{x}, \tag{3.20}$$

which is the Reynolds–Orr equation for the evolution of the kinetic energy of the velocity perturbation $\boldsymbol{u}$. We now proceed to bound the inertial terms on the right-hand side of (3.20) by the dissipative terms.

3.2.1. *The Newtonian fluid region, Ω_1*

We note that the perturbed velocity field satisfies $\boldsymbol{u} = 0$ at the interface Γ_i, where $r = r_i$. For such velocity fields, substituting from (3.1) for $W(r)$, the terms on the right-hand side of (3.20) become

$$[\text{Inertia}] \; + \; [\text{Dissipation}] = \frac{B}{m r_y} \int_{\Omega_1} r u_r w \, \mathrm{d}\boldsymbol{x} - \frac{m}{Re^{[2]}} \int_{\Omega_1} \left[\frac{\partial u_i}{\partial x_j} \right]^2 \mathrm{d}\boldsymbol{x}. \quad (3.21)$$

We now write

$$\int_{\Omega_1} r u_r w \, \mathrm{d}\boldsymbol{x} \leqslant \Lambda_N \int_{\Omega_1} \left[\frac{\partial u_i}{\partial x_j} \right]^2 \mathrm{d}\boldsymbol{x}, \quad (3.22)$$

where

$$\Lambda_N \equiv \sup_{\tilde{\boldsymbol{u}} \in \bar{V}_{N,0}} \frac{\displaystyle\int_{\Omega_1} r \tilde{u}_r \tilde{w} \, \mathrm{d}\boldsymbol{x}}{\displaystyle\int_{\Omega_1} \left| \frac{\partial \tilde{u}_i}{\partial x_j} \right|^2 \mathrm{d}\boldsymbol{x}}. \quad (3.23)$$

The test space $\bar{V}_{N,0}$, above, is the closure of $V_{N,0}$, with respect to the $[H^1(\Omega_1)]^3$ norm. The space $V_{N,0}$ consists of functions that satisfy the following conditions:

(*a*) $\tilde{\boldsymbol{u}} \in C^\infty(\Omega_1)$,
(*b*) $\tilde{\boldsymbol{u}}$ is solenoidal, i.e. $\partial \tilde{u}_j / \partial x_j = 0$,
(*c*) $\tilde{\boldsymbol{u}} = 0$ on Γ_i,
(*d*) $\tilde{\boldsymbol{u}}$ is periodic in z.

By the simple mapping: $\boldsymbol{x} = r_i \tilde{\boldsymbol{x}}$, we can transform (3.23) into an equivalent problem on the unit cylinder. This problem has been solved by Joseph & Carmi (1969), in their classical work on absolute stability of Hagen–Poiseuille flow. Using Joseph & Carmi's solution we have

$$\int_{\Omega_1} r u_r w \, \mathrm{d}\boldsymbol{x} \leqslant \frac{r_i^3}{R_J} \int_{\Omega_1} \left[\frac{\partial u_i}{\partial x_j} \right]^2 \mathrm{d}\boldsymbol{x}, \quad (3.24)$$

where $R_J = 81.49$, i.e. $\Lambda_N \leqslant r_i^3 / R_J$.

3.2.2. *The Bingham fluid region, Ω_2*

Following the analysis in Nouar & Frigaard (2001), substituting for $W(r)$, and by considering pointwise the integrand in the dissipative term on the right-hand side of (3.20), we may write

$$\begin{aligned} [\text{Inertia}] \; + \; [\text{Dissipation}] \; &= \; - \int_{\Omega_2} u_r \frac{\partial W}{\partial r} w + \frac{1}{Re^{[2]}} \frac{\partial u_i}{\partial x_j} \left[{\tau_{ij}}^{[2]}(\boldsymbol{U} + \boldsymbol{u}) - {\tau_{ij}}^{[2]}(\boldsymbol{U}) \right] \mathrm{d}\boldsymbol{x}, \\ &\leqslant \; \frac{B}{r_y} \int_{\Omega_2 :\; r \geqslant r_y} (r - r_y) u_r w \, \mathrm{d}\boldsymbol{x} - \frac{1}{Re^{[2]}} \int_{\Omega_2} \dot{\gamma}(\boldsymbol{u})^2 \, \mathrm{d}\boldsymbol{x}. \quad (3.25) \end{aligned}$$

Condition (3.13), with a selected to satisfy (3.14), guarantees that there will be an unyielded plug region surrounding the Newtonian region in the perturbed flow. Thus, we may assume the existence of some thickness, $h = h(r_i, B, m) > 0$, such that the perturbed flow remains unyielded for $r \in (r_i, r_i + h)$. We define $\Omega_{2,p}$ to be this plug

region:

$$\Omega_{2,p} = \{\boldsymbol{x} : r \in (r_i, r_i + h)\}. \tag{3.26}$$

Note that both terms in (3.25) will have zero contribution within $\Omega_{2,p}$. Thus, in considering the domain $\Omega_2|\Omega_{2,p}$, at the boundary with $\Omega_{2,p}$ we have both $\dot{\gamma}_{ij}(\boldsymbol{u}) = 0$ and $\boldsymbol{u} = 0$ (since here we have assumed stationary domains). Thus, we can write (3.25) as

$$[\text{l.h.s. (3.25)}] \leqslant \frac{B}{r_y} \int_{\Omega_2|\Omega_{2,p}} [r - (r_i + h) + g(r)] u_r w \, \mathrm{d}\boldsymbol{x} - \frac{1}{Re^{[2]}} \int_{\Omega_2|\Omega_{2,p}} \left[\frac{\partial u_i}{\partial x_j}\right]^2 \mathrm{d}\boldsymbol{x}, \tag{3.27}$$

where $g(r)$ is defined by

$$g(r) = \begin{cases} r_i + h - r_y, & r > r_y, \\ r_i + h - r, & r \in [r_i + h, r_y]. \end{cases} \tag{3.28}$$

We bound the two parts of the inertial term separately:

$$[\text{Inertia}] \leqslant \frac{B}{r_y} [\Lambda_B + (r_y - r_i - h)\Lambda_C] \int_{\Omega_2|\Omega_{2,p}} \left[\frac{\partial u_i}{\partial x_j}\right]^2 \mathrm{d}\boldsymbol{x}, \tag{3.29}$$

where

$$(\Lambda_B, \Lambda_C) \equiv \sup_{\tilde{\boldsymbol{u}} \in \bar{V}_{B,0}} \left(\frac{\displaystyle\int_{\Omega_2|\Omega_{2,p}} [r - (r_i + h)] \tilde{u}_r \tilde{w} \, \mathrm{d}\boldsymbol{x}}{\displaystyle\int_{\Omega_2|\Omega_{2,p}} \left|\frac{\partial \tilde{u}_i}{\partial x_j}\right|^2 \mathrm{d}\boldsymbol{x}}, \frac{\displaystyle\int_{\Omega_2|\Omega_{2,p}} |\tilde{u}_r \tilde{w}| \, \mathrm{d}\boldsymbol{x}}{\displaystyle\int_{\Omega_2|\Omega_{2,p}} \left|\frac{\partial \tilde{u}_i}{\partial x_j}\right|^2 \mathrm{d}\boldsymbol{x}} \right). \tag{3.30}$$

The test space $\bar{V}_{B,0}$, above, is the closure of $V_{B,0}$, with respect to the $[H^1(\Omega_2|\Omega_{2,p})]^3$ norm, where $V_{B,0}$ contains functions satisfying

(*a*) $\tilde{\boldsymbol{u}} \in C^\infty(\Omega_2|\Omega_{2,p})$,
(*b*) $\tilde{\boldsymbol{u}}$ is solenoidal, i.e. $\partial \tilde{u}_j / \partial x_j = 0$,
(*c*) $\tilde{\boldsymbol{u}} = 0$ on the walls of the pipe,
(*d*) $\tilde{\boldsymbol{u}}$ is periodic in z,
(*e*) $\dot{\gamma}_{ij}(\tilde{\boldsymbol{u}}) = 0$ at the boundary with $\Omega_{2,p}$,
(*f*) $\tilde{\boldsymbol{u}} = 0$ at the boundary with $\Omega_{2,p}$.

Although we can find the constants Λ_B and Λ_C by solving appropriate eigenvalue problems, we instead simply search for simple analytical upper bounds for Λ_B and Λ_C. These upper bounds will correspond to lower bounds on the Reynolds numbers required for stability, i.e. the actual stability will be better than the bounds we present. To this end, we introduce the transformation

$$z = \tilde{z}[1 - (r_i + h)], \qquad r - (r_i + h) = \tilde{r}[1 - (r_i + h)].$$

We map functions in $V_{B,0}$ onto the unit cylinder $\tilde{r} \in [0, 1]$, say $\tilde{\Omega}$. By virtue of conditions (*e*) and (*f*), each function that we map onto $\tilde{\Omega}$ will be continuous and differentiable at $\tilde{r} = 0$. We now bound above, by relaxing conditions (*e*) and (*f*) and considering instead $\tilde{\bar{V}}_{B,0}$, the closure of $\tilde{V}_{B,0}$, which is the space of functions on $\tilde{\Omega}$ satisfying

(*a*) $\tilde{\boldsymbol{u}} \in C^\infty(\tilde{\Omega})$,
(*b*) $\tilde{\boldsymbol{u}}$ is solenoidal,
(*c*) $\tilde{\boldsymbol{u}} = 0$ at $\tilde{r} = 1$,
(*d*) $\tilde{\boldsymbol{u}}$ is periodic in $\tilde{z}$.

Thus, we have

$$(\Lambda_B, \Lambda_C) \leqslant \sup_{\tilde{\boldsymbol{u}} \in \tilde{\bar{V}}_{B,0}} \left([1-(r_i+h)]^3 \frac{\int_{\tilde{\Omega}} \tilde{r}\tilde{u}_r \tilde{w}\, \mathrm{d}\tilde{\boldsymbol{x}}}{\int_{\tilde{\Omega}} \left| \frac{\partial \tilde{u}_i}{\partial \tilde{x}_j} \right|^2 \mathrm{d}\tilde{\boldsymbol{x}}}, [1-(r_i+h)]^2 \frac{\int_{\tilde{\Omega}} |\tilde{u}_r \tilde{w}|\, \mathrm{d}\tilde{\boldsymbol{x}}}{\int_{\tilde{\Omega}} \left| \frac{\partial \tilde{u}_i}{\partial \tilde{x}_j} \right|^2 \mathrm{d}\tilde{\boldsymbol{x}}} \right)$$
$$= \left(\frac{[1-(r_i+h)]^3}{R_J}, \frac{[1-(r_i+h)]^2}{R_M} \right), \tag{3.31}$$

where R_J is again Joseph & Carmi's constant, and R_M is another constant independent of the problem parameters. It is obvious that $R_M < R_J$ and we can easily derive the estimate $R_M \geqslant 5.78319$, following the procedure in § 4.3.5. Since this constant is not used explicitly in what follows, we have not attempted a more accurate evaluation.

3.3. *Stability bounds*

Combining the above bounds, we have straightforwardly

$$\frac{1}{2}\frac{D}{Dt}\int_{\Omega} \boldsymbol{u}^2\, \mathrm{d}\boldsymbol{x} \leqslant \left(\frac{B[\Lambda_B + (r_y - r_i - h)\Lambda_C]}{r_y} - \frac{1}{Re^{[2]}} \right) \int_{\Omega_2} \left| \frac{\partial u_i}{\partial x_j} \right|^2 \mathrm{d}\boldsymbol{x}$$
$$+ \left(\frac{B\Lambda_N}{m r_y} - \frac{m}{Re^{[2]}} \right) \int_{\Omega_1} \left| \frac{\partial u_i}{\partial x_j} \right|^2 \mathrm{d}\boldsymbol{x}. \tag{3.32}$$

We suppose that the following condition holds:

$$Re^{[2]} < \min \left\{ \frac{r_y}{B[\Lambda_B + (r_y - r_i - h)\Lambda_C]}, \frac{r_y m^2}{B\Lambda_N} \right\}. \tag{3.33}$$

We can bound (3.32) above as follows:

$$\frac{1}{2}\frac{\mathrm{d}}{\mathrm{d}t}\int_{\Omega} \frac{u_i^2}{2}\, \mathrm{d}\boldsymbol{x} \leqslant -\lambda c_P \int_{\Omega} \boldsymbol{u}^2\, \mathrm{d}\boldsymbol{x}, \tag{3.34}$$

where

$$\lambda = \min \left\{ \left(\frac{1}{Re^{[2]}} - \frac{B[\Lambda_B + (r_y - r_i - h)\Lambda_C]}{r_y} \right), \left(\frac{m}{Re^{[2]}} - \frac{B\Lambda_N}{m r_y} \right) \right\} \tag{3.35}$$

and where c_P is the relevant constant from the Poincaré inequality. Hence, the following energy stability bound holds for the exponential decay of $\|\boldsymbol{u}\|^2_{L^2(\Omega)}$:

$$\|\boldsymbol{u}\|^2_{L^2(\Omega)}(t) \leqslant \|\boldsymbol{u}\|^2_{L^2(\Omega)}(0) \exp^{-2c_P \lambda t}. \tag{3.36}$$

In order to explore (3.33), we insert the bounds on $(\Lambda_N, \Lambda_B, \Lambda_C)$ from (3.24) and (3.31). By setting $r = r_i + h$ in (3.14), and reducing $a_{\max}(r_i, B, m) \to 0$ we also have $r_i + h \to r_y$. Thus, by selection of an appropriate $a_{\max}(r_i, B, m)$ we can take $(r_y - r_i - h)$ as small as we like (obviously this also makes our conditional stress bound $a < a_{\max}(r_i, B, m)$ weaker). For simplicity we now select $a_{\max}(r_i, B, m)$ so that we can choose h to satisfy

$$r_y - r_i - h = (1 - r_i - h)\frac{R_M}{R_J} < 1,$$

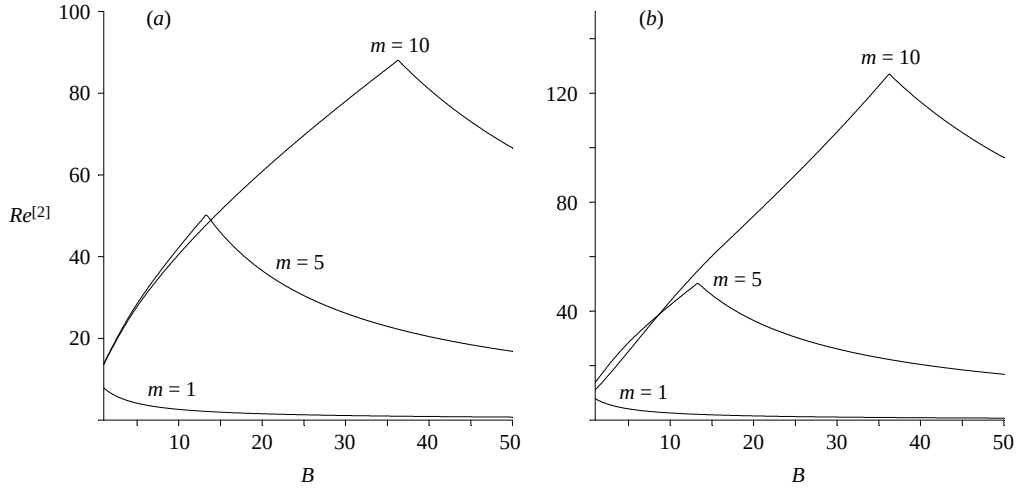

FIGURE 5. Exploration of the approximate bound (3.38) for nonlinear stability, $Re_c^{[2]}$. variations with B and m: (*a*) $r_i = 0.5$, (*b*) $r_i = 0.7$.

so that the two bounds in (3.31) coincide. We find that the flow is conditionally nonlinearly stable for

$$Re^{[2]} < 81.49 \min\left\{\frac{m^2 r_y}{B r_i^3}, \frac{r_y}{2B(1-r_i-h)^3}\right\}, \tag{3.37}$$

which is simpler to analyse. Assuming as above that $a_{\max}(r_i, B, m)$ is small, we have that $r_i + h \approx r_y$, and thus we explore the approximate bound

$$Re^{[2]} \lessapprox Re_c^{[2]} = 81.49 \frac{r_y}{B} \min\left\{\frac{m^2}{r_i^3}, \frac{1}{2(1-r_y)^3}\right\}, \tag{3.38}$$

which depends only on (B, r_i, m), i.e. the same parameters as the basic flow. We plot the stability limit (3.38) in figure 5 for various values of viscosity ratio m and different r_i. For increasing m and at moderate values of B, we are clearly able to achieve nonlinear stability at moderately large values of $Re^{[2]}$.

Figure 5 is best understood in the context of transitions the basic flow solutions. Certainly, some of the features shown in figure 5 are physically intuitive. For $m > 1$ the Newtonian fluid is more viscous than the lubricating Bingham fluid and thus we observe that either increasing the viscosity ratio m further or increasing the amount of Newtonian fluid (i.e. r_i) both increase the stability of the flow. Note that the total flow rate is fixed.

The variation with B appears peculiar: first the stability bounds increase, then decrease. The decrease is certainly counter-intuitive, contradicts linear stability behaviour found in Frigaard (2001), and requires some explanation. At small B we generally have a fully yielded (case 2) basic flow, see figure 4, and the above analysis is anyway invalid. As B increases we have transition to case 1 solutions, where Ω_1 is surrounded by unyielded fluid and our results are valid. Further increases in B result in the yielded fluid region narrowing and an increase in the second term in (3.38), which is the active bound. Thus, we see the expected increase in stability with B. The second term in (3.38) approaches infinity as B increases. Thus, at some point the first term in (3.38) becomes active (at this point the maximal

bounds in figure 5 are attained), and thereafter the stability bounds decrease. The decrease occurs because r_y/B decreases. The ring of yielded Bingham fluid becomes progressively narrower and the flow rate of Bingham fluid decreases. Since the total flow rate is conserved, the flow rate of Newtonian fluid must increase. This requires an increased pressure drop (and note that $r_y/B \propto 1/|P_z|$). Eventually (and this is beyond the Bingham number range shown in figure 5), transition to a case 3 solution occurs. The Newtonian fluid is then flowing through a wholly unyielded annulus and r_y/B becomes constant, i.e. the curves in figure 5 all asymptote to a constant positive value at large B.

4. Moving Ω_1

We now turn to the general problem in which the Newtonian region may move. Our results will be derived under the assumption that for small finite perturbations away from the axisymmetric flow and for a bounded stress perturbation satisfying (3.13), an annular region of thickness at least h will remain about Ω_1. Since there is no deformation within the plug, the shape of the interface Γ_i remains circular of radius r_i, but Ω_1 may move. Thus, $\Omega_1(t)$ is a cylinder of radius r_i, which at time t has axis centred at $\boldsymbol{x}_c(t) = (x_c(t), y_c(t), 0)$. We show later that the departure from axisymmetry,

$$r_c(t) \equiv |(x_c(t), y_c(t))|, \tag{4.1}$$

can be bounded under suitable assumptions on the Reynolds number.

Movement of the Newtonian region represents the first complication that must be dealt with. The second complication concerns the choice of basic flow that we consider for the perturbation. In deriving nonlinear stability bounds, we must consider quantities such as

$$\frac{\partial u_i}{\partial x_j}\left[{\tau_{ij}}^{[k]}(\boldsymbol{U}+\boldsymbol{u}) - {\tau_{ij}}^{[k]}(\boldsymbol{U})\right].$$

If the interface between fluids moves, but a fixed basic flow is considered, it will happen that certain points $\boldsymbol{x}$ are in fluid 1 for the perturbed flow but are in fluid 2 for the basic flow. Since there is a jump in the rheology between fluids, this presents a problem in deriving meaningful nonlinear† stability bounds for multi-phase systems. To circumvent this key difficulty, we consider perturbations about a basic flow solution that is not fixed in time. Instead we consider perturbed velocity and pressure fields of the following form:

$$\boldsymbol{U}+\boldsymbol{u} = (0, 0, W(x, y; x_c(t), y_c(t)) + (u, v, w), \qquad P(z; x_c(t), y_c(t)) + p,$$

where the basic flow is parameterized by (x_c, y_c). This particular basic flow corresponds to the axial flow solution for a two-fluid system in which Ω_1 is a circular region of radius r_i, centred at (x_c, y_c). We consider these solutions in depth in §4.2. First, we show that consideration of the flow as a perturbation about these basic flows leads only to a minor change in the energy stability problem.

† Note that in a linear analysis this problem is not encountered. Here it is common practice to linearize about the basic flow interface, effectively extending the basic solution on one side of an interface into the fluid on the other side. For a nonlinear perturbation, this procedure is not admissible.

4.1. *Derivation of the Reynolds–Orr equation*

For the basic and perturbed flows, at time t the fluid domains are $\Omega_1(t)$ and $\Omega_2(t)$. The following equations are satisfied in fluid k:

$$0 = -\frac{\partial P}{\partial x_i} + \frac{1}{Re^{[2]}}\frac{\partial}{\partial x_j}\tau_{ij}{}^{[k]}(\boldsymbol{U}), \tag{4.2}$$

$$0 = \frac{\partial U_i}{\partial x_i}, \tag{4.3}$$

$$\left[\frac{\partial}{\partial t} + (U_j + u_j)\frac{\partial}{\partial x_j}\right](U_i + u_i) = -\frac{\partial}{\partial x_i}(P + p) + \frac{1}{Re^{[2]}}\frac{\partial}{\partial x_j}\tau_{ij}{}^{[k]}(\boldsymbol{U} + \boldsymbol{u}), \tag{4.4}$$

$$0 = \frac{\partial}{\partial x_i}(U_i + u_i). \tag{4.5}$$

We note that the basic solution $(\boldsymbol{U}, P)$ is still a full solution to the steady Navier–Stokes equations, but is not itself steady, i.e. in the sense that $\boldsymbol{x}_c = \boldsymbol{x}_c(t)$ and also because strictly speaking, in considering a time-varying solution, (4.2)–(4.3) are not really the equations of steady motion. However, even though time dependent, $(\boldsymbol{U}, P)$ are a solution of (4.2)–(4.3) at time t.

The point $\boldsymbol{x}_c(t)$ is moving with speed $\boldsymbol{u}_c(t) = (u_c(t), v_c(t), 0)$, given by

$$u_c(t) = \frac{\mathrm{d}x_c}{\mathrm{d}t}(t), \qquad v_c(t) = \frac{\mathrm{d}y_c}{\mathrm{d}t}(t). \tag{4.6}$$

This allows us to rewrite (4.4) as follows:

$$\left[\frac{\partial}{\partial t} + (U_j + u_j)\frac{\partial}{\partial x_j}\right]u_i + u_j\frac{\partial U_i}{\partial x_j} = -\frac{\partial}{\partial x_i}(P + p) + \frac{1}{Re^{[2]}}\frac{\partial}{\partial x_j}\tau_{ij}{}^{[k]}(\boldsymbol{U} + \boldsymbol{u}) - \delta_{i3}[\boldsymbol{u}_c \cdot \nabla_c W], \tag{4.7}$$

noting that $U_j \partial U_i/\partial x_j = 0$. Here ∇_c denotes the gradient operator, with respect to the variables $\boldsymbol{x}_c$. We subtract (4.2) from (4.7), multiply by u_i, and integrate over the individual fluid domains, at time t. We then sum the two fluid domain Reynolds–Orr equations, eliminating the boundary integrals, giving the following Reynolds–Orr equation:

$$\frac{\mathrm{d}}{\mathrm{d}t}\sum_k \int_{\Omega_k} \frac{u_i^2}{2}\,\mathrm{d}\boldsymbol{x} = -\sum_k \int_{\Omega_k}\left[u_j\frac{\partial W}{\partial x_j} + \boldsymbol{u}_c \cdot \nabla_c W\right] w\,\mathrm{d}\boldsymbol{x} - \frac{1}{Re^{[2]}}\sum_k \int_{\Omega_k}\frac{\partial u_i}{\partial x_j}\left[\tau_{ij}{}^{[k]}(\boldsymbol{U} + \boldsymbol{u}) - \tau_{ij}{}^{[k]}(\boldsymbol{U})\right]\mathrm{d}\boldsymbol{x}. \tag{4.8}$$

We note that this differs from (3.20) only in the additional terms involving $[\boldsymbol{u}_c \cdot \nabla_c W]$. These additional terms are the trade-off for ensuring that the perturbed and basic flow regions coincide at time t. Although marginally more complex, we can still analyse (4.8) to derive stability bounds (see § 4.3). However, this approach only makes sense if the basic flows $(\boldsymbol{U}(x_c, y_c), P(x_c, y_c))$ are well-defined for all values of (x_c, y_c), and if also the plug region persists in these flows for sufficiently small r_c.

4.2. *The basic flows* (W, P_z).

The basic flows (W, P_z) are defined as solutions to the axial flow problem:

$$Re^{[2]}\frac{\partial P}{\partial z} = \frac{\partial \tau_{zx}{}^{[k]}}{\partial x} + \frac{\partial \tau_{zy}{}^{[k]}}{\partial y}, \quad (x, y) \in \Omega_k,\ k = 1, 2, \tag{4.9}$$

where Ω_1 is an infinitely long circular cylinder of radius r_i, with axis centred at $(x, y) = (x_c, y_c)$. The problem is two-dimensional in the (x, y)-plane. In the Newtonian region,

$$\frac{\partial \tau_{zx}{}^{[1]}}{\partial x} + \frac{\partial \tau_{zy}{}^{[1]}}{\partial y} = m\left(\frac{\partial^2 W}{\partial x^2} + \frac{\partial^2 W}{\partial y^2}\right),$$

and in the Bingham region, the constitutive laws simplify to

$$|\nabla W| = 0 \Longleftrightarrow \left[(\tau_{zx})^{[2]})^2 + (\tau_{zy})^{[2]})^2\right]^{1/2} \leqslant B, \tag{4.10}$$

$$\left(\tau_{zx}^{[2]}, \tau_{zy}^{[2]}\right) = \left[1 + \frac{B}{|\nabla W|}\right] \nabla W \Longleftrightarrow \left[(\tau_{zx})^{[2]})^2 + (\tau_{zy})^{[2]})^2\right]^{1/2} > B. \tag{4.11}$$

No-slip conditions are satisfied at the wall: both the traction and velocity are continuous at the interface. The axial pressure gradient is a constant, determined by the following flow rate constraint:

$$\pi = \int_{x^2+y^2<1} W(x, y)\, \mathrm{d}x\, \mathrm{d}y. \tag{4.12}$$

The question of existence of (W, P_z) is addressed in Frigaard & Scherzer (1998). For each interface (i.e. here each pair (x_c, y_c)), there exists a unique weak solution W for given fixed P_z. The flow rate is shown in Frigaard & Scherzer (1998) to increase monotonically with $|P_z|$, and thus (4.12) can be used to find the unique pressure gradient, P_z. Thus, for each (x_c, y_c) we have a unique solution (W, P_z). Since Ω_1 is a circular cylinder, these solutions will only be unique up to a rotational symmetry about the pipe axis, i.e. they depend on r_c rather than (x_c, y_c). If $r_c \geqslant 1 - r_i$, then Ω_1 touches the pipe wall. There still exists a basic solution (W, P_z), but we are not able to preserve an unyielded plug region surrounding Ω_1. Therefore, it is immediately clear that we must somehow bound r_c in order to preserve the plug.

For $r_c = 0$, the solution (W, P_z) corresponds to the axisymmetric flow of § 3.1. We suppose a parameter choice such that we have a case 1 solution, (i.e. figures 1*c*, 3*a*), so that r_y is found as the solution of (3.2). The shear stress is given by $\tau_{rz}^{[2]} = -Br/r_y$ and the pressure gradient is $P_z(r_c = 0) = -2B/(r_y Re^{[2]})$. The flow is axisymmetric, hence $\tau_{\theta z} = 0$ everywhere and $\tau = |\tau_{rz}^{[2]}| = Br/r_y$. Thus, at the interface

$$\tau = \frac{Br_i}{r_y}, \tag{4.13}$$

i.e. the larger the initial annulus of unyielded fluid, the further below the yield stress is the interfacial stress, and the more likely that the plug region is preserved.

Now consider small $r_c \neq 0$. If the plug region is preserved then in Ω_1, W satisfies

$$\nabla^2 W = -\frac{Re^{[2]}}{m}\frac{\partial P}{\partial z}(r_c). \tag{4.14}$$

It is reasonable expect that the pressure gradient varies continuously with r_c. The boundary conditions for W in (4.14) are that $W = W_p$ at the interface, where W_p is the plug velocity. Thus, $W - W_p$ satisfies Poisson's equation with Dirichlet boundary conditions on Ω_1, for which there is a unique solution. Furthermore, this unique solution is axisymmetric, i.e. about (x_c, y_c), depending only on $r' = [(x - x_c)^2 + (y - y_c)^2]^{1/2}$. Therefore, if the plug region is intact, inside the Newtonian domain we have

$$\tau_{r'z} = Re^{[2]}\frac{r}{2}\frac{\partial P}{\partial z}(r_c), \qquad \tau_{\theta' z} = 0,$$

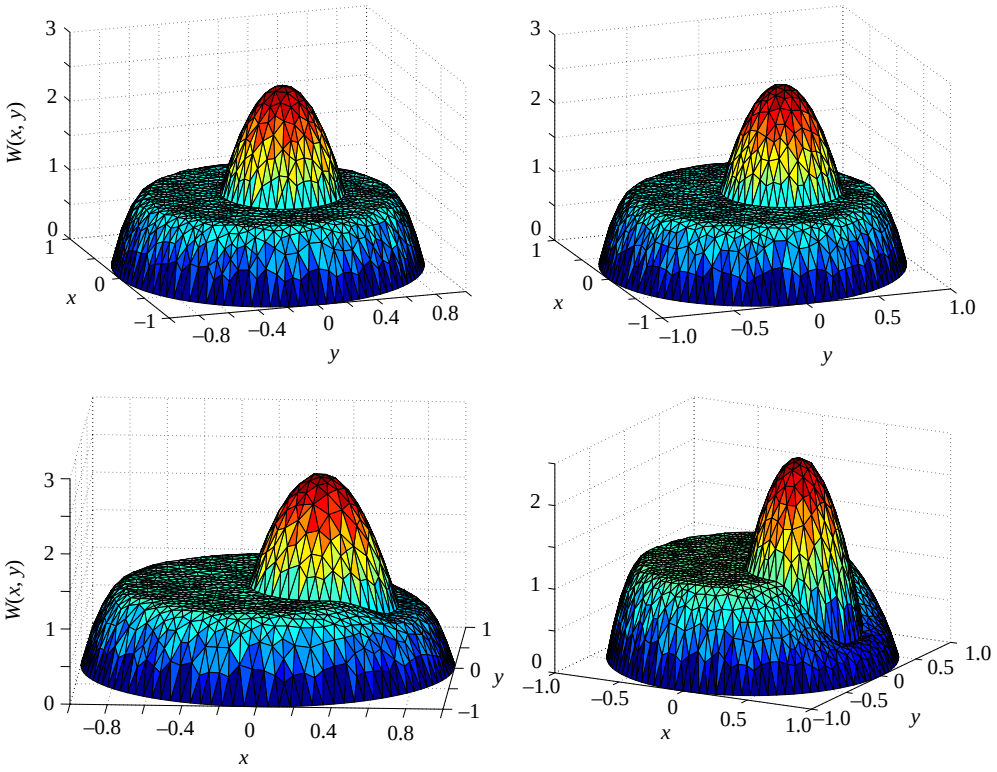

FIGURE 6. Asymmetric basic flow: $B = 30$, $m = 2$, $r_i = 0.4$ (cf. figure 3 (*a*): (*a*) $(x_c, y_c) = (0.1, 0)$; (*b*) $(x_c, y_c) = (0.2, 0)$; (*c*) $(x_c, y_c) = (0.3, 0)$; (*d*) $(x_c, y_c) = (0.4, 0)$.

where θ' is an azimuthal coordinate centred at (x_c, y_c). Continuity of stress ensures that $\tau_{r'z}$ is continuous at the interface $r' = r_i$. Thus, if P_z varies continuously with r_c and if $|\tau_{\theta' z}|$ varies continuously from its values at $r_c = 0$, (i.e. from zero), then $\tau^{[2]} < B$ at the interface for some finite range of sufficiently small r_c. Thus, by simple continuity arguments we can assert that the plug region is preserved.

In order to evaluate the limit of r_c for which the plug region is preserved, it is necessary to compute (W, P_z). For this we have used an augmented Lagrangian approach. Such algorithms were developed approximately 20 years ago for visco-plastic fluid flows, see Glowinski, Lions & Trémolières (1981), Fortin & Glowinski (1983), Glowinski (1984). Although these have been occasionally used, e.g. Hoppe *et al.* (1999), Huilgol & Pannizza (1995), Saramito & Roquet (2001), Vola, Boscardin & Latché (2003), most researchers appear to currently favour using regularized viscosity approaches. Augmented Lagrangian approaches avoid the problems of non-differentiability of the yield stress term in the dissipation functional, by using relaxation. In this way, they are able to compute unyielded regions correctly. Details of the numerical method we use are in Moyers-Gonzalez & Frigaard (2003). Briefly, we adapt the algorithm ALG2, described in Fortin & Glowinski (1983), Glowinski (1984), in a straightforward manner to deal with the two fluids, and implement using a finite element method with piecewise linear elements on triangles. Convergence is tested by using the axisymmetric flow of § 3.1 as a test problem.

To illustrate the effects of increasing r_c from zero, we present a sequence of solutions with the same parameters as in figure 3(*a*), but for $r_c = 0.1,\ 0.2,\ 0.3,\ 0.4$ (figure 6).

We can see that the plug is still preserved in a ring around Ω_1 for $r_c = 0.2$, but breaks before $r_c = 0.3$, as Ω_1 nears the pipe wall. Although time consuming, it would be possible to iteratively determine the critical value of r_c at which the plug first breaks at the interface, Γ_i. Additionally, at each r_c, one could compute the maximal unyielded concentric annular plug width about Ω_1.

4.3. *Three-dimensional nonlinear stability bounds*

We turn now to the analysis of (4.8), which we write as

$$\begin{aligned}
\frac{\mathrm{d}}{\mathrm{d}t}\sum_k \int_{\Omega_k} \frac{u_i^2}{2}\,\mathrm{d}\boldsymbol{x} &= -\frac{1}{Re^{[2]}}\int_{\Omega_2} \frac{\partial u_i}{\partial x_j}\left[{\tau_{ij}}^{[2]}(\boldsymbol{U}+\boldsymbol{u}) - {\tau_{ij}}^{[2]}(\boldsymbol{U})\right]\mathrm{d}\boldsymbol{x} && \text{(Term A)},\\
&\quad -\int_{\Omega_2}\left[u\frac{\partial W}{\partial x} + v\frac{\partial W}{\partial y} + \frac{\partial W}{\partial x_c}u_c + \frac{\partial W}{\partial y_c}v_c\right] w\,\mathrm{d}\boldsymbol{x} && \text{(Term B)},\\
&\quad -\frac{1}{Re^{[2]}}\int_{\Omega_1} \frac{\partial u_i}{\partial x_j}\left[{\tau_{ij}}^{[1]}(\boldsymbol{U}+\boldsymbol{u}) - {\tau_{ij}}^{[1]}(\boldsymbol{U})\right]\mathrm{d}\boldsymbol{x} && \text{(Term C)},\\
&\quad -\int_{\Omega_1}\left[u\frac{\partial W}{\partial x} + v\frac{\partial W}{\partial y} + \frac{\partial W}{\partial x_c}u_c + \frac{\partial W}{\partial y_c}v_c\right] w\,\mathrm{d}\boldsymbol{x} && \text{(Term D)},
\end{aligned} \tag{4.15}$$

and examine each of terms A–D separately. Our aim is not to establish the best possible bounds, since this problem is complicated significantly by the asymmetric geometry, but instead to establish that an energy stability bound exists. We then use this to bound the departure of the flow from axisymmetry (in § 4.3.4), i.e. so that we can restrict r_c to be arbitrarily small.

4.3.1. *The Bingham fluid region, $\Omega_2(t)$*

We treat first the Bingham fluid region. We suppose that $\Omega_1(t)$ is surrounded by a region of Bingham fluid of finite width, within which both the basic flow and the perturbed flow are unyielded. To formalize this, suppose that for $r_c < b_1$, all asymmetric basic flows have a finite width of unyielded plug, see e.g. figure 7. We now impose a bound of form (3.13) on the stress perturbations, i.e.

$$\left|{\tau_{ij}}^{[k]}(\boldsymbol{U}+\boldsymbol{u}) - {\tau_{ij}}^{[k]}(\boldsymbol{U})\right| < b_2, \qquad k = 1, 2;\ i, j = 1, 2, 3. \tag{4.16}$$

As in § 3.2, by taking b_2 suitably small, but finite, the plug will persist for the perturbation, within a finite range. We combine these conditions, by assuming that if $r_c < b_1$ and b_2 is suitably chosen, then there exists $h = h(b_1, b_2) > 0$ such that

$$\dot{\gamma}_{ij}(\boldsymbol{u}) = \dot{\gamma}_{ij}(\boldsymbol{U}) = 0: \qquad \forall (x, y):\ r_i < [(x - x_c)^2 + (y - y_c)^2]^{1/2} < r_i + h. \tag{4.17}$$

We denote by $\Omega_{2,p}(t)$ this ring of unyielded plug surrounding $\Omega_1(t)$, see figure 7(*a*). The plug is treated as a rigid body. Since we consider an infinitely long pipe, rotational movements of the plug region are only possible about axes that are parallel to the z-axis. Thus, at time t, the plug motion can be described as combination of a linear motion, say $(u_c, v_c, w_c + W_p)$, and a rigid body rotation about an axis through $(x_c(t), y_c(t), 0)$, parallel to the z-axis. Recall that (u_c, v_c) is the speed of $(x_c(t), y_c(t))$, and here W_p denotes the speed of the plug region in the basic flow. Let

$$\boldsymbol{u}^* = (u^*, v^*, w^*) \equiv (u_c, v_c, w_c) + (-(y - y_c)\tilde{\omega}_c, (x - x_c)\tilde{\omega}_c, 0), \tag{4.18}$$

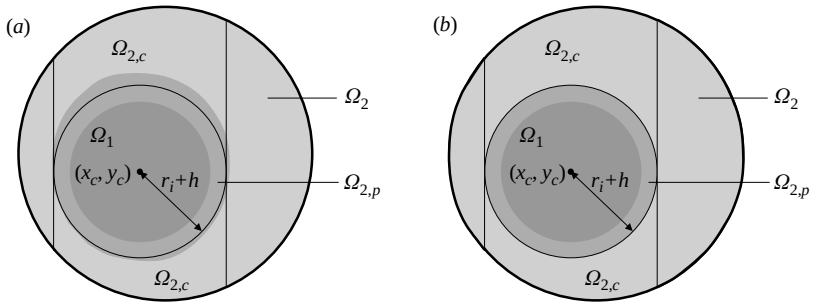

FIGURE 7. (*a*) Geometry of the perturbed flow; (*b*) definition of the domain $\Omega_{2,c}$.

where $\tilde{\omega}_c(t)$ denotes the instantaneous rotation of the plug about the z-axis through $(x_c(t), y_c(t))$. Thus, for any $\boldsymbol{x} \in \Omega_{2,p}(t)$, $\boldsymbol{u}^* + \boldsymbol{U}$, gives exactly the perturbed velocity of the fluid in the rigid plug and $\boldsymbol{u}^* = \boldsymbol{u}$. Turning to term A, we proceed as before:

$$\begin{aligned}(\text{Term A}) &= -\frac{1}{Re^{[2]}} \int_{\Omega_2} \frac{\partial u_i}{\partial x_j} \left[\tau_{ij}{}^{[2]}(\boldsymbol{U}+\boldsymbol{u}) - \tau_{ij}{}^{[2]}(\boldsymbol{U})\right] \mathrm{d}\boldsymbol{x} \\ &\leqslant -\frac{1}{Re^{[2]}} \int_{\Omega_2 | \Omega_{2,p}} \dot{\gamma}(\boldsymbol{u})^2 \,\mathrm{d}\boldsymbol{x} = -\frac{1}{Re^{[2]}} \int_{\Omega_2} \dot{\gamma}(\boldsymbol{u})^2 \,\mathrm{d}\boldsymbol{x} \\ &= -\frac{1}{Re^{[2]}} \int_{\Omega_2} \left|\frac{\partial u_i}{\partial x_j}\right|^2 - \frac{2\pi L (r_i \tilde{\omega}_c)^2}{Re^{[2]}}. \end{aligned} \tag{4.19}$$

To derive the last line above from the second line, we have used the divergence theorem and substituted from (4.18) to evaluate the (non-vanishing) boundary integral at Γ_i. This gives rise to the rotational term above. Thus, rotation of the plug region increases the dissipation, as might be expected.

For the inertial term B in (4.15), we note that $\partial W/\partial x = \partial W/\partial y = 0$ if $\boldsymbol{x} \in \Omega_{2,p}$. We define $|\nabla W|_{2,\max}$ and $|\nabla_c W|_{\max}$ by

$$\max_{(x,y)\in\Omega_2|\Omega_{2,p}} |\nabla W| = |\nabla W|_{2,\max}, \tag{4.20}$$

$$\max_{|(x_c,y_c)|<b;\ (x,y)\in\Omega_2|\Omega_{2,p}} |\nabla_c W| = |\nabla_c W|_{\max}. \tag{4.21}$$

To bound u_c and v_c, we use (4.18) to write, for $|x - x_c| < (r_i + h)$,

$$2u_c = u\big(x,\, y_c - ((r_i+h)^2 - (x-x_c)^2)^{1/2}, z\big) + u\big(x,\, y_c + ((r_i+h)^2 - (x-x_c)^2)^{1/2}, z\big), \tag{4.22}$$

and a similar expression for v_c, i.e. we use the values of u and v at opposite points on the boundary of the unyielded plug/interface, to cancel out rotational terms in (4.18). We now replace u with an integral of its partial derivative, integrated outwards to the wall in the domain $\Omega_{2,c}$ (as defined in figure 7*b*), i.e. for $u(x, y_c - ((r_i+h)^2 - (x-x_c)^2)^{1/2}, z)$ we write

$$u\big(x,\, y_c - ((r_i+h)^2 - (x-x_c)^2)^{1/2}, z\big) = \int_{-1-x^2}^{y_c - ((r_i+h)^2-(x-x_c)^2)^{1/2}} \frac{\partial u}{\partial y}(x, y, z)\,\mathrm{d}y,$$

and an analogous expression for $u(x, y_c + ((r_i+h)^2 - (x-x_c)^2)^{1/2}, z)$ (integrated upwards in the upper part of $\Omega_{2,c}$). We now integrate (4.22) with respect to x over the

range $|x - x_c| < (r_i + h)$, and use the above expression, to give the following bound:

$$2u_c(r_i + h)L \leqslant \int_{\Omega_{2,c}} \left|\frac{\partial u}{\partial y}\right| \mathrm{d}\boldsymbol{x}, \leqslant \int_{\Omega_2|\Omega_{2,p}} \left|\frac{\partial u}{\partial y}\right| \mathrm{d}\boldsymbol{x},$$
$$\leqslant [\pi(1-(r_i+h)^2)L]^{1/2}\left[\int_{\Omega_2|\Omega_{2,p}} \left|\frac{\partial u}{\partial y}\right|^2 \mathrm{d}\boldsymbol{x}\right]^{1/2} \tag{4.23}$$

(also using the Cauchy–Schwarz inequality). Similarly, we have

$$2v_c(r_i + h)L \leqslant [\pi(1-(r_i+h)^2)L]^{1/2}\left[\int_{\Omega_2|\Omega_{2,p}} \left|\frac{\partial v}{\partial x}\right|^2 \mathrm{d}\boldsymbol{x}\right]^{1/2}. \tag{4.24}$$

Now let $(\Lambda_{B,1}, \Lambda_{B,2})$, be defined as follows:

$$(\Lambda_{B,1}, \Lambda_{B,2}) \equiv \sup_{\tilde{\boldsymbol{u}}\in\bar{V}_{B,0}} \left(\frac{\displaystyle\int_{\Omega_2|\Omega_{2,p}} (\tilde{u}+\tilde{v})\tilde{w}\,\mathrm{d}\boldsymbol{x}}{\displaystyle\int_{\Omega_2|\Omega_{2,p}} \left|\frac{\partial \tilde{u}_i}{\partial x_j}\right|^2 \mathrm{d}\boldsymbol{x}}, \frac{\displaystyle\int_{\Omega_2} \tilde{w}^2\,\mathrm{d}\boldsymbol{x}}{\displaystyle\int_{\Omega_2} \left|\frac{\partial \tilde{u}_i}{\partial x_j}\right|^2 \mathrm{d}\boldsymbol{x}} \right). \tag{4.25}$$

The test space $\bar{V}_{B,0}$ above is the closure of $V_{B,0}$, which is as defined in § 3.2.2, except that we remove condition (f), i.e. we allow movement of Ω_1. Combining all the above bounds, terms A and B of (4.15) satisfy

$$(\text{Term A}) + (\text{Term B}) \leqslant \left[A_B - \frac{1}{Re^{[2]}}\right] \int_{\Omega_2} \left|\frac{\partial u_i}{\partial x_j}\right|^2 \mathrm{d}\boldsymbol{x} - \frac{2\pi L(r_i\tilde{\omega}_c)^2}{Re^{[2]}}, \tag{4.26}$$

where

$$A_B = |\nabla W|_{2,\max}\Lambda_{B,1} + \frac{\pi|\nabla_c W|_{\max}(1-(r_i+h)^2)^{1/2}\left(1-r_i^2\right)^{1/2}\Lambda_{B,2}^{1/2}}{\sqrt{2}(r_i+h)}. \tag{4.27}$$

4.3.2. *The Newtonian fluid region, $\Omega_1(t)$*

We turn now to terms C and D in (4.15), dealing first with the dissipative term. Consider the velocity field $\boldsymbol{u}'$, defined by

$$\boldsymbol{u}' = \boldsymbol{u} - \boldsymbol{u}^*. \tag{4.28}$$

We note the following:

(i) Since $\boldsymbol{u}^*$ is the perturbation of the plug velocity in $\Omega_{2,p}$ and the velocity is continuous across the interface, at $[(x-x_c)^2 + (y-y_c)^2]^{1/2} = r_i$, it follows that

$$\boldsymbol{u}' = 0, \qquad \boldsymbol{x} \in \partial\Omega_1(t). \tag{4.29}$$

(ii) Since $\boldsymbol{u}^*$ consists of only a linear translation and a rigid body rotation

$$\dot{\gamma}_{ij}(\boldsymbol{u}^*) = 0, \qquad \text{and therefore} \qquad \dot{\gamma}_{ij}(\boldsymbol{u}) = \dot{\gamma}_{ij}(\boldsymbol{u}'). \tag{4.30}$$

Using the above, the dissipative term in (4.15) on $\Omega_1(t)$ is

$$-(\text{Term C}) = \frac{m}{Re^{[2]}}\int_{\Omega_1} \dot{\gamma}(\boldsymbol{u})^2\,\mathrm{d}\boldsymbol{x} = \frac{m}{Re^{[2]}}\int_{\Omega_1} \dot{\gamma}(\boldsymbol{u}')^2\,\mathrm{d}\boldsymbol{x} = \frac{m}{Re^{[2]}}\int_{\Omega_1} \left|\frac{\partial u_i'}{\partial x_j}\right|^2 \mathrm{d}\boldsymbol{x}. \tag{4.31}$$

We now introduce (4.28) into the inertial term in (4.15) on $\Omega_1(t)$:

$$\text{(Term D)} = -\int_{\Omega_1}\left[(u'+u^*)\frac{\partial W}{\partial x}+(v'+v^*)\frac{\partial W}{\partial y}+\frac{\partial W}{\partial x_c}u_c+\frac{\partial W}{\partial y_c}v_c\right](w'+w_c)\,\mathrm{d}\boldsymbol{x},$$

and expand to give

$$\begin{aligned}\text{(Term D)} = &-\int_{\Omega_1}\left[u'\frac{\partial W}{\partial x}+v'\frac{\partial W}{\partial y}\right]w'+\left[u_c\left(\frac{\partial W}{\partial x}+\frac{\partial W}{\partial x_c}\right)+v_c\left(\frac{\partial W}{\partial y}+\frac{\partial W}{\partial y_c}\right)\right]w'\,\mathrm{d}\boldsymbol{x}\\ &-\int_{\Omega_1}\left[(y-y_c)\tilde{\omega}_c\frac{\partial W}{\partial x}-(x-x_c)\tilde{\omega}_c\frac{\partial W}{\partial y}\right]w'+\left[u'\frac{\partial W}{\partial x}+v'\frac{\partial W}{\partial y}\right]w_c\,\mathrm{d}\boldsymbol{x}\\ &-\int_{\Omega_1}\left[u_c\left(\frac{\partial W}{\partial x}+\frac{\partial W}{\partial x_c}\right)+v_c\left(\frac{\partial W}{\partial y}+\frac{\partial W}{\partial y_c}\right)\right]w_c\,\mathrm{d}\boldsymbol{x}\\ &-\int_{\Omega_1}\left[(y-y_c)\tilde{\omega}_c\frac{\partial W}{\partial x}-(x-x_c)\tilde{\omega}_c\frac{\partial W}{\partial y}\right]w_c\,\mathrm{d}\boldsymbol{x}. \qquad (4.32)\end{aligned}$$

In order to bound the above expressions, we need first to find bounds for both w_c and $\tilde{\omega}_c$. At time t we define a cylindrical coordinate system (r',θ'), centred at $(x_c(t), y_c(t))$. Now w_c is the perturbation of the axial component of the plug velocity, and is constant. In terms of the (r',θ') coordinate system, the outer wall of the pipe is denoted by $r' = r_o(\theta')$. We have the following:

$$\begin{aligned}2\pi L(r_i+h)w_c &= (r_i+h)\int_{-L/2}^{L/2}\int_0^{2\pi} w_c(\theta')\,\mathrm{d}\theta'\mathrm{d}z\\ &\leqslant \int_{-L/2}^{L/2}\int_0^{2\pi}\int_{r_i+h}^{r_o(\theta')}\left|\frac{\partial w}{\partial r'}\right|r'\,\mathrm{d}r'\mathrm{d}\theta'\mathrm{d}z = \int_{\Omega_2|\Omega_{2,p}}\left|\frac{\partial w}{\partial r'}\right|\,\mathrm{d}\boldsymbol{x}\\ &\leqslant [\pi(1-(r_i+h)^2)L]^{1/2}\left[\int_{\Omega_2|\Omega_{2,p}}\left|\frac{\partial u_i}{\partial x_j}\right|^2\mathrm{d}\boldsymbol{x}\right]^{1/2}. \qquad (4.33)\end{aligned}$$

To bound $\tilde{\omega}_c$ we again use (4.18) to write, for $|x-x_c|<(r_i+h)$,

$$2\tilde{\omega}_c((r_i+h)^2-(x-x_c)^2)^{1/2} = u\big(x,\, y_c-((r_i+h)^2-(x-x_c)^2)^{1/2},\, z\big) \qquad (4.34)$$

$$-u\big(x,\, y_c+((r_i+h)^2-(x-x_c)^2)^{1/2},\, z\big), \qquad (4.35)$$

and we can derive an analogous expression using values of v. As before, we write $u(x, y_c-((r_i+h)^2-(x-x_c)^2)^{1/2}, z)$ and $u(x, y_c+((r_i+h)^2-(x-x_c)^2)^{1/2}, z)$ in terms of integrals of $\partial u/\partial y$, and integrate (4.34) between $x_c \pm (r_i+h)$. Performing similar operations with our expression involving v, and combining, we derive

$$|\tilde{\omega}_c| \leqslant \frac{(1-(r_i+h)^2)^{1/2}}{(2\pi L)^{1/2}(r_i+h)^2}\left[\int_{\Omega_2|\Omega_{2,p}}\left|\frac{\partial u_i}{\partial x_j}\right|^2\mathrm{d}\boldsymbol{x}\right]^{1/2}; \qquad (4.36)$$

further details may be found in Moyers-Gonzalez (2002).

We now consider upper bounds for the individual terms in (4.32). We first note that if Ω_1 is surrounded by a region of unyielded Bingham fluid, then the basic flow W is such that $W = W(r')$, and furthermore, for $\boldsymbol{x} \in \Omega_1$,

$$W(r') = W_{N,\max}\left[1-\left(\frac{r'}{r_i}\right)^2\right]+W_p \Longrightarrow \left|\frac{\mathrm{d}W}{\mathrm{d}r'}\right| = \frac{2W_{N,\max}}{r_i^2}r'.$$

Now let $\boldsymbol{\Lambda}_N = (\Lambda_{N,1}, \Lambda_{N,2}, \Lambda_{N,3}, \Lambda_{N,4})$, be defined as follows:

$$\boldsymbol{\Lambda}_N \equiv \sup_{\tilde{\boldsymbol{u}} \in \bar{V}_{N,0}} \left(\frac{\displaystyle\int_{\Omega_1} r' \tilde{u}_{r'} \tilde{w} \, \mathrm{d}\boldsymbol{x}}{\displaystyle\int_{\Omega_1} \left| \frac{\partial \tilde{u}_i}{\partial x_j} \right|^2 \mathrm{d}\boldsymbol{x}}, \frac{\displaystyle\int_{\Omega_1} [r' \tilde{w}]^2 \, \mathrm{d}\boldsymbol{x}}{\displaystyle\int_{\Omega_1} \left| \frac{\partial \tilde{u}_i}{\partial x_j} \right|^2 \mathrm{d}\boldsymbol{x}}, \frac{\displaystyle\int_{\Omega_1} \tilde{w}^2 \, \mathrm{d}\boldsymbol{x}}{\displaystyle\int_{\Omega_1} \left| \frac{\partial \tilde{u}_i}{\partial x_j} \right|^2 \mathrm{d}\boldsymbol{x}}, \frac{\displaystyle\int_{\Omega_1} [r' \tilde{u}_{r'}]^2 \, \mathrm{d}\boldsymbol{x}}{\displaystyle\int_{\Omega_1} \left| \frac{\partial \tilde{u}_i}{\partial x_j} \right|^2 \mathrm{d}\boldsymbol{x}} \right), \tag{4.37}$$

where $\tilde{u}_{r'}$ is the radial component of $\tilde{\boldsymbol{u}}$, i.e. in the direction of r'. The test space $\bar{V}_{N,0}$ above is as defined previously. Finally, we have for (4.32)

$$\begin{aligned}
(\text{Term D}) \leqslant\ & \frac{2W_{N,\max}\Lambda_{N,1}}{r_i^2} \int_{\Omega_1} \left| \frac{\partial u_i'}{\partial x_j} \right|^2 \mathrm{d}\boldsymbol{x} + \left[\frac{\pi W_{N,\max}[2\Lambda_{N,2}(1-(r_i+h)^2)]^{1/2}}{r_i(r_i+h)} \right. \\
& \left. + \frac{\pi |\nabla_c W|_{\max} r_i [2\Lambda_{N,3}(1-(r_i+h)^2)]^{1/2}}{r_i+h} + \frac{W_{N,\max}[\Lambda_{N,4}(1-(r_i+h)^2)]^{1/2}}{r_i(r_i+h)} \right] \\
& \times \left[\int_{\Omega_1} \left| \frac{\partial u_i'}{\partial x_j} \right|^2 \mathrm{d}\boldsymbol{x} \right]^{1/2} \left[\int_{\Omega_2 | \Omega_{2,p}} \left| \frac{\partial u_i}{\partial x_j} \right|^2 \mathrm{d}\boldsymbol{x} \right]^{1/2} \\
& + \left[\frac{\pi r_i W_{N,\max}(1-(r_i+h)^2)}{3\sqrt{2}(r_i+h)^2} + \frac{\pi r_i^2 |\nabla_c W|_{\max}(1-(r_i+h)^2)}{2\sqrt{2}(r_i+h)^2} \right] \\
& \times \int_{\Omega_2 | \Omega_{2,p}} \left| \frac{\partial u_i}{\partial x_j} \right|^2 \mathrm{d}\boldsymbol{x}.
\end{aligned} \tag{4.38}$$

We now combine the above bounds for terms C and D in (4.15):

$$\begin{aligned}
(\text{Term C}) + (\text{Term D}) \leqslant\ & A_N \int_{\Omega_2 | \Omega_{2,p}} \left| \frac{\partial u_i}{\partial x_j} \right|^2 \mathrm{d}\boldsymbol{x} + C_N \int_{\Omega_1} \left| \frac{\partial u_i'}{\partial x_j} \right|^2 \mathrm{d}\boldsymbol{x} \\
& + 2B_N \left[\int_{\Omega_1} \left| \frac{\partial u_i'}{\partial x_j} \right|^2 \mathrm{d}\boldsymbol{x} \right]^{1/2} \left[\int_{\Omega_2 | \Omega_{2,p}} \left| \frac{\partial u_i}{\partial x_j} \right|^2 \mathrm{d}\boldsymbol{x} \right]^{1/2} \\
& - \frac{m}{Re^{[2]}} \int_{\Omega_1} \left| \frac{\partial u_i'}{\partial x_j} \right|^2 \mathrm{d}\boldsymbol{x}
\end{aligned} \tag{4.39}$$

$$\leqslant (A_N + B_N) \int_{\Omega_2} \left| \frac{\partial u_i}{\partial x_j} \right|^2 \mathrm{d}\boldsymbol{x} + \left(B_N + C_N - \frac{m}{Re^{[2]}} \right) \int_{\Omega_1} \left| \frac{\partial u_i'}{\partial x_j} \right|^2 \mathrm{d}\boldsymbol{x}, \tag{4.40}$$

where A_N, B_N and C_N are the positive parameters

$$A_N = \frac{\pi r_i^2 (1-(r_i+h)^2)}{\sqrt{2}(r_i+h)^2} \left[\frac{W_{N,\max}}{3r_i} + \frac{|\nabla_c W|_{\max}}{2} \right], \tag{4.41}$$

$$B_N = \frac{\pi (1-(r_i+h)^2)^{1/2}}{\sqrt{2} r_i (r_i+h)} \left[W_{N,\max} \Lambda_{N,2}^{1/2} + |\nabla_c W|_{\max} r_i^2 \Lambda_{N,3}^{1/2} + W_{N,\max} [2\Lambda_{N,4}]^{1/2} \right], \tag{4.42}$$

$$C_N = \frac{2W_{N,\max}\Lambda_{N,1}}{r_i^2}; \tag{4.43}$$

further details may be found in Moyers-Gonzalez (2002).

4.3.3. *The stability bound*

We combine (4.15) with the bounds (4.26) and (4.40):

$$\frac{1}{2}\frac{\mathrm{d}}{\mathrm{d}t}\int_{\Omega}\boldsymbol{u}^2\,\mathrm{d}\boldsymbol{x} \leqslant \left(A_N + B_N + A_B - \frac{1}{Re^{[2]}}\right)\int_{\Omega_2}\left|\frac{\partial u_i}{\partial x_j}\right|^2\mathrm{d}\boldsymbol{x} - \frac{2\pi L(r_i\tilde{\omega}_c)^2}{Re^{[2]}} + \left(B_N + C_N - \frac{m}{Re^{[2]}}\right)\int_{\Omega_1}\left|\frac{\partial u_i'}{\partial x_j}\right|^2\mathrm{d}\boldsymbol{x}. \tag{4.44}$$

Suppose the following condition holds, (for nonlinear stability):

$$Re^{[2]} < \min\left\{\frac{1}{A_N + B_N + A_B}, \frac{m}{B_N + C_N}\right\}. \tag{4.45}$$

Assuming (4.45), we ignore the $(\tilde{\omega}_c)^2$ term in (4.44) and have

$$\begin{aligned}\frac{1}{2}\frac{\mathrm{d}}{\mathrm{d}t}\int_{\Omega}\boldsymbol{u}^2\,\mathrm{d}\boldsymbol{x} &\leqslant -\lambda\int_{\Omega}\dot{\gamma}(\boldsymbol{u})^2\,\mathrm{d}\boldsymbol{x}\\ &\leqslant -c\lambda\int_{\Omega}\boldsymbol{u}^2\,\mathrm{d}\boldsymbol{x},\end{aligned} \tag{4.46}$$

where

$$\lambda = \min\left\{\left(\frac{1}{Re^{[2]}} - A_N - B_N - A_B\right), \left(\frac{m}{Re^{[2]}} - B_N - C_N\right)\right\}. \tag{4.47}$$

In deriving (4.46) we have used Korn's inequality on Ω (see e.g. Duvaut & Lions 1976, p. 110), with c the resulting constant. Hence, under the condition (4.45), the following energy stability bound holds for the decay of $\|\boldsymbol{u}\|^2_{L^2(\Omega)}(t)$:

$$\|\boldsymbol{u}\|^2_{L^2(\Omega)}(t) \leqslant \|\boldsymbol{u}\|^2_{L^2(\Omega)}(0)\exp^{-2c\lambda t}. \tag{4.48}$$

Note precisely what this means. When $\|\boldsymbol{u}\|^2_{L^2(\Omega)}(t)\to 0$ the perturbation decays to zero, but we have perturbed about an asymmetric basic flow, i.e. the perturbed flow does not decay to the axisymmetric basic flow, but instead to a different basic flow, which is in fact unknown. It remains to see if this asymmetric basic flow is close to the axisymmetric flow. For this we consider how large $r_c(t)$ may become when (4.45) holds.

4.3.4. *A bound for r_c*

We have assumed throughout that $r_c < b_1$, which we now verify can be satisfied for arbitrary $b_1 > 0$. First note that, for an initially concentric interface, (x_c, y_c) satisfy the following initial value problem:

$$\frac{\mathrm{d}}{\mathrm{d}t}(x_c, y_c) = (u_c, v_c), \qquad (x_c, y_c)(0) = (0, 0). \tag{4.49}$$

To bound u_c and v_c, we use (4.18) again, and note that for any $r' \in (r_i, r_i + h)$

$$2u_c = u\big(x, y_c - ((r')^2 - (x - x_c)^2)^{1/2}, z\big) + u\big(x, y_c + ((r')^2 - (x - x_c)^2)^{1/2}, z\big), \tag{4.50}$$

for $|x - x_c| < r'$ (and similarly for v_c). On integrating over $\Omega_{2,p}$ and using (4.48)

$$\begin{aligned}u_c L\pi\big[(r_i + h)^2 - r_i^2\big] &= \int_{\Omega_{2,p}} u\mathrm{d}\boldsymbol{x} \leqslant \big(L\pi\big[(r_i + h)^2 - r_i^2\big]\big)^{1/2}\left[\int_{\Omega} u^2\mathrm{d}\boldsymbol{x}\right]^{1/2},\\ |u_c|(t) &\leqslant \frac{\|\boldsymbol{u}\|_{L^2(\Omega)}(0)}{\big(L\pi\big[(r_i + h)^2 - r_i^2\big]\big)^{1/2}}\exp^{-c\lambda t},\end{aligned} \tag{4.51}$$

with the identical bound for $|v_c|(t)$. We now integrate (4.49) with respect to t and use the bounds on $|u_c|(t)$ and $|v_c|(t)$, to give

$$|x_c|(t) \leqslant \int_0^\infty |u_c|(t)\mathrm{d}t \leqslant \frac{\|\boldsymbol{u}\|_{L^2(\Omega)}(0)}{c\lambda(L\pi[(r_i+h)^2 - r_i^2])^{1/2}}, \quad |y_c|(t) \leqslant \frac{\|\boldsymbol{u}\|_{L^2(\Omega)}(0)}{c\lambda(L\pi[(r_i+h)^2 - r_i^2])^{1/2}}. \tag{4.52}$$

Thus, finally we have

$$r_c(t) = |(x_c, y_c)|(t) \leqslant \frac{\sqrt{2}\|\boldsymbol{u}\|_{L^2(\Omega)}(0)}{c\lambda\left(L\pi\left[(r_i+h)^2 - r_i^2\right]\right)^{1/2}} \quad \forall t \geqslant 0. \tag{4.53}$$

Thus, by choosing $\|\boldsymbol{u}\|_{L^2(\Omega)}(0)$ sufficiently small we can ensure that $r_c < b_1$, for arbitrary small finite b_1. Note too that an initial bound on $\|\boldsymbol{u}\|_{L^2(\Omega)}(0)$ is achieved by taking b_2 sufficiently small in (4.16), i.e. bounding the stress perturbation bounds the integral of $\dot{\gamma}(\boldsymbol{u})^2$, which via Korn's inequality bounds $\|\boldsymbol{u}\|_{L^2(\Omega)}(0)$.

4.3.5. *Evaluation of the parameters contributing to the stability bounds*

Whereas it was fairly easy in § 3.3 to understand the variations in stability with the parameters that define the basic flow, here it is much harder. Since we consider only bounded $r_c < b$, and our basic solutions depend on (x_c, y_c), B, m, and r_i, we may assume that the constants $|\nabla W|_{2,max}$, $|\nabla_c W|_{max}$, $W_{N,max}$ are well defined provided that $W(x, y; x_c, y_c)$ is differentiable with respect to each of the above parameters, which is reasonable. It is a large computational task to determine the parametric variation of each of these constants with each parameter describing the basic flow. From the computations that we have performed, $W_{N,max}$ appears to increase with both B and r_i, but decreases with m, and is bounded above. The parameter $|\nabla W|_{2,max}$ is generally $O(1)$. To compute $|\nabla_c W|_{max}$ is very time consuming and we have not attempted this. We note however that $W = O(1)$, since the velocity is scaled with the mean value and the flow rate constraint is always satisfied. Thus, changing (x_c, y_c) will simply increase W in some parts of the domain whilst decreasing W in other parts. It is therefore assumed that $|\nabla_c W|_{max}$ is numerically of $O(1)$ and fairly insensitive to changes in B, m, and r_i.

Constants such as $\Lambda_{B,1}$ and $\Lambda_{B,2}$ can be computed as the smallest positive eigenvalues of an eigenvalue problem, via the Euler–Lagrange equations for the different minimization problems. In the case that $(x_c, y_c) = (0, 0)$, for all t (i.e. the Newtonian region does not move), we have already considered the much simpler problem and derived approximate bounds (see § 3.2.2). In general, it is hard to progress with sharp bounds for $\Lambda_{B,1}$ and $\Lambda_{B,2}$ when the asymmetric case is considered, due to the shape of $\Omega_2|\Omega_{2,p}$ and the large number of parameters involved in a computational study. However, we can at least establish that $\Lambda_{B,1}$ and $\Lambda_{B,2}$ are well defined, as follows. We know that

$$|w| \leqslant \int_{R_i+h}^{r'_w(\theta')} \left|\frac{\partial w}{\partial r'}\right| \mathrm{d}r' \leqslant \frac{1}{(R_i+h)^{1/2}} \int_{R_i+h}^{r'_w(\theta')} r'^{1/2} \left|\frac{\partial w}{\partial r'}\right| \mathrm{d}r', \tag{4.54}$$

where $r'_w(\theta')$ denotes the radial distance to the pipe wall from (x_c, y_c). Now,

$$\int_{\Omega_2|\Omega_{2,p}} w^2 \mathrm{d}\boldsymbol{x} \leqslant \iiint_{R_i+h}^{r'_w(\theta')} \frac{r'_w(\theta')}{(R_i+h)} \left[\int_{R_i+h}^{r'_w(\theta')} r''^{1/2} \left|\frac{\partial w}{\partial r''}\right| \mathrm{d}r''\right]^2 \mathrm{d}r'\mathrm{d}\theta'\mathrm{d}z.$$

Using the Cauchy–Schwarz inequality we get

$$\int_{\Omega_2|\Omega_{2,p}} w^2 \mathrm{d}\boldsymbol{x} \leqslant \iint \frac{2-(R_i+h)}{(R_i+h)}[r'_w(\theta')-(R_i+h)]^2 \int_{R_i+h}^{r'_w(\theta')} r'' \left(\left|\frac{\partial w}{\partial r''}\right|\right)^2 \mathrm{d}r''\mathrm{d}\theta'\mathrm{d}z.$$

Applying the mean value theorem for integrals,

$$\int_{\Omega_2|\Omega_{2,p}} w^2 \mathrm{d}\boldsymbol{x} \leqslant \frac{2-(R_i+h)}{(R_i+h)}[r'_w(\theta'^*)-(R_i+h)]^2 \int_{\Omega_2|\Omega_{2,p}} \left(\left|\frac{\partial w}{\partial r''}\right|\right)^2 \mathrm{d}\boldsymbol{x},$$

but

$$\int_{\Omega_2|\Omega_{2,p}} \left(\left|\frac{\partial u_i}{\partial x_j}\right|\right)^2 \mathrm{d}\boldsymbol{x} \geqslant \int_{\Omega_2|\Omega_{2,p}} \left(\left|\frac{\partial w}{\partial r''}\right|\right)^2 \mathrm{d}\boldsymbol{x}. \tag{4.55}$$

Therefore, we have that

$$\Lambda_{B,2} \leqslant \frac{2-(R_i+h)}{(R_i+h)}[r'_w(\theta'^*)-(R_i+h)]^2. \tag{4.56}$$

Similarly, for $\Lambda_{B,1}$ we can derive

$$\Lambda_{B,1} \leqslant \frac{\displaystyle\int_{\Omega_2|\Omega_{2,p}} (u+v)w \,\mathrm{d}\boldsymbol{x}}{\displaystyle\int_{\Omega_2|\Omega_{2,p}} \left(\left|\frac{\partial u_i}{\partial x_j}\right|\right)^2 \mathrm{d}\boldsymbol{x}} \leqslant 2\left(\frac{2-(R_i+h)}{(R_i+h)}[r'_w(\theta'^*)-(R_i+h)]^2\right). \tag{4.57}$$

This establishes that $\Lambda_{B,1}$ and $\Lambda_{B,2}$ are well-defined. Our bounds are very conservative.

Estimates for $\Lambda_{N,1}$, $\Lambda_{N,2}$, $\Lambda_{N,3}$, $\Lambda_{N,4}$ are much easier due to the circular domain and homogeneous Dirichlet conditions. Again each parameter can be defined via an eigenvalue problem for a different set of Euler–Lagrange equations, which could be solved computationally. Instead, here we just establish that these bounds exist and then give an upper estimate for the bounds. For simplicity we map the Newtonian region into the unit circle, which simplifies the dependence on r_i. The bound for $\Lambda_{N,1}$ is due to Joseph & Carmi (1969):

$$\Lambda_{N,1} \leqslant \frac{r_i^3}{81.49}, \tag{4.58}$$

and believed to be exact. For $\Lambda_{N,2}$, $\Lambda_{N,3}$, $\Lambda_{N,4}$, we simply relax the constraints in the definition of these bounds, as follows:

$$(\Lambda_{N,2}, \Lambda_{N,3}, \Lambda_{N,4}) \leqslant \sup_{\tilde{\boldsymbol{u}}\in\bar{V}_{N,0}} \left(\frac{\displaystyle\int_{\Omega_1}[r'\tilde{w}]^2 \,\mathrm{d}\boldsymbol{x}}{\displaystyle\int_{\Omega_1}\left|\frac{\partial\tilde{w}}{\partial r}\right|^2 \mathrm{d}\boldsymbol{x}}, \frac{\displaystyle\int_{\Omega_1}\tilde{w}^2 \,\mathrm{d}\boldsymbol{x}}{\displaystyle\int_{\Omega_1}\left|\frac{\partial\tilde{w}}{\partial r}\right|^2 \mathrm{d}\boldsymbol{x}}, \frac{\displaystyle\int_{\Omega_1}[r'\tilde{u}_{r'}]^2 \,\mathrm{d}\boldsymbol{x}}{\displaystyle\int_{\Omega_1}\left|\frac{\partial\tilde{u}_{r'}}{\partial r}\right|^2 \mathrm{d}\boldsymbol{x}}\right). \tag{4.59}$$

Note that, by eliminating the additional terms in the denominators, we are effectively throwing away the divergence-free condition, but can now deal with decoupled problems, the solutions of which involve the least positive roots of the Bessel function of zeroth order, J_0 (details are omitted):

$$(\Lambda_{N,2}, \Lambda_{N,3}, \Lambda_{N,4}) \leqslant \left(\frac{r_i^4}{23.13275}, \frac{r_i^2}{5.78319}, \frac{r_i^4}{23.13275}\right). \tag{4.60}$$

These bounds for $\Lambda_{N,2}$, $\Lambda_{N,3}$, $\Lambda_{N,4}$ are also likely to be fairly conservative.

5. Conclusions

In this paper we have considered the nonlinear stability of a multi-layer shear flow, and established stability bounds under quite general conditions. These are the only results of this type that we know of, and this seems to be promising as a practical method for establishing multi-layer flows in industrial applications. In this context, the next step is clearly to provide an experimental demonstration, and for this purpose an apparatus is already under construction. If we consider flows with a static wall layer (e.g. figure 3(*c*), stable displacement flows are reported in Gabard (2001), Gabard & Hulin (2003). In these experiments a yield stress fluid (Carbopol) initially occupies a circular tube. It is displaced by injecting a purely viscous fluid, which forms a stable finger in the centre of the tube, leaving the yield stress fluid at rest on the walls. Consequently, we are reasonably confident that we can achieve in practice the multi-layer flows that we have investigated here.

In § 3 we have shown that our method can yield stable Reynolds numbers of the same order as found in nonlinear stability studies of Newtonian fluids. Such methods are known to be fairly conservative and it is likely that significantly larger Reynolds numbers will also be nonlinearly stable. The limitation of the results in § 3 is that the stress perturbations must be assumed to be axisymmetric, which occurs in perturbations that are close to being linear. In any practical application one would attempt to avoid asymmetries in the flow and suppress initial perturbations as far as possible, i.e. one would not want the Newtonian region to hit the wall of the pipe. Thus, the best possible bounds that we are likely to achieve in practice are those associated with the axisymmetric flow in § 3. In deriving the more general bounds in § 4, the complexity becomes prohibitive and we are forced to make many conservative assumptions. Thus, numerical values of the Reynolds numbers required for stability are typically $O(1)$. However, we would expect bounds on stability to be continuous with the axisymmetric stability bounds as the departure from asymmetry approaches zero. Hence, the problem to study further in order to improve the bounds is the simpler problem in § 3. The value of the analysis in § 4 is simply to show that, even without symmetry, nonlinear stability bounds can be derived.

The methodology that we have used in § 4 is perhaps of independent interest. Our problem is one of relatively few non-trivial multi-fluid flows for which energy stability bounds have been successfully employed, and it is worthwhile outlining those features of our analysis which have allowed this.

(i) We assume throughout that there is a conditional bound on the stress perturbation. The origin of this idea is in Frigaard (2001) and in Nouar & Frigaard (2001). Here it serves two purposes. First it allows the elimination of interfacial instabilities, since the interface can move but not deform, cf. Frigaard (2001). Second, it allows the derivation of stability bounds on a restricted domain, cf. Nouar & Frigaard (2001), which is how the Bingham number enters into the analysis, and the eventual stability bounds. These ideas are specific to a visco-plastic fluid.

(ii) We perturb about an arbitrary asymmetric basic flow. This idea is not specific to a visco-plastic fluid and could be used elsewhere, although we are unaware of its application to other problems. To make absolutely transparent the value of this, consider two Newtonian fluids in a nonlinear stability analysis. If we fix the basic flow and allow that in certain regions the fluid type of basic and perturbed flows may change, then the dissipative terms contain contributions such as

$$-\tfrac{1}{2}\left[\tau_{ij}{}^{[1]}(\boldsymbol{U}+\boldsymbol{u})-\tau_{ij}{}^{[2]}(\boldsymbol{U})\right]\dot{\gamma}_{ij}(\boldsymbol{u})=-\mu^{[1]}\dot{\gamma}^2(\boldsymbol{u})-\left(\mu^{[1]}-\mu^{[2]}\right)\tfrac{1}{2}\dot{\gamma}_{ij}(\boldsymbol{U})\dot{\gamma}_{ij}(\boldsymbol{u}).$$

Although the first term on the right-hand side above is negative (i.e. dissipative) the second term could be positive or negative; similar problems arise with the indices reversed. This is a significant problem with the straightforward application of energy methods to multi-fluid problems. Use of our method would not be generally applicable. Typically, for a given interface projection onto the (x, y)-plane, one can find an axial solution to the multi-fluid problem. However, for purely viscous fluids this becomes less relevant since the entire interface deforms. The yield stress allows the structure of the flow to be preserved.

(iii) We allow movement of the fluid regions, but then derive a bound for that movement. This too is facilitated by the fluids having a yield stress. The plug velocity has a relatively simple description which can be related to the motion of the Newtonian region. Thus, our energy bound allows us to bound the movement of Ω_1. This part of our methodology might be applicable to certain two-phase fluid–solid problems. One analogy would be to consider, for example, an iso-density solid immersed in the plug region of a Bingham fluid Hagen–Poiseuille flow. Since visco-plastic suspensions are often used for the transport of particles (e.g. in rock cuttings transported by drilling mud in the oil industry, coal–water slurries, etc.), such studies may have practical value.

Our future work in this area is undecided, since there are a number of interesting avenues for exploration. Experimentally, we are working towards a demonstration of these flows and then an experimental study, which we hope to report. We are also interested in extensions of the methodology that we have introduced. In this context, more realistic visco-plastic fluids and the inclusion of small density differences are of primary interest, practically speaking. More broadly, many complex fluids are both visco-elastic and visco-plastic. We might consider whether the inherent stability of our visco-plastically lubricated flow could be used to compensate for certain of the visco-elastic instabilities commonly observed. Eventually, this might be the area of primary application of this type of flow.

The contribution of M. A. M.-G. has been supported through a graduate scholarship from Consejo Nacional de Ciencia y Tecnología (CONACYT) of Mexico, held at University of British Columbia. The research of I. A. F. is supported by NSERC Canada and the British Columbia Advanced Systems Institute (BCASI), through the award of a BCASI university research fellowship. The contribution of C. N. has been made during a sabbatical visit to the University of British Columbia, supported financially by CNRS France and partly by NSERC & BCASI. The support of our sponsors is gratefully acknowledged. We thank the referees for their comments and guidance in shortening the original version.

REFERENCES

Allouche, M., Frigaard, I. A. & Sona, G. 2000 Static wall layers in the displacement of two visco-plastic fluids in a plane channel. *J. Fluid Mech.* **424**, 243–277.

Bittleston, S. H. & Hassager, O. 1992 Flow of visco-plastic fluids in a rotating concentric annulus. *J. Non-Newtonian Fluid Mech.* **42**, 19–36.

Charru, F. 1998 "Phase diagram" of interfacial instabilities in two-layer shear flows. *Proc. Third Intl Conf. on Multiphase Flow, ICMF'98, Lyon, France, June 8–12, 1998.*

Charru, F. & Hinch, E. J. 2000 "Phase diagram" of interfacial instabilities in a two-layer Couette flow and mechanism of the long wave instability. *J. Fluid Mech.* **414**, 195–223.

Drazin, P. G. & Reid, W. H. 1981 *Hydrodynamic Stability*. Cambridge University Press.

Duvaut, G. & Lions, J.-L. 1976 *Inequalities in Mechanics and Physics*, p. 219. Springer.

Fortin, M. & Glowinski, R. 1983 *Augmented Lagrangian Methods : Applications to the Numerical Solution of Boundary-value Problems*. North Holland.

Frigaard, I. A. 2001 Super-stable parallel flows of multiple visco-plastic fluids. *J. Non-Newtonian Fluid Mech.* **100**, 49–76.

Frigaard, I. A., Howison, S. D. & Sobey, I. J. 1994 On the stability of Poiseuille flow of a Bingham Fluid. *J. Fluid. Mech.* **263**, 133–150.

Frigaard, I. A., Leimgruber, S. & Scherzer, O. 2003 Variational methods and maximal residual wall layers. *J. Fluid Mech.* **483**, 37–65.

Frigaard, I. A. & Scherzer, O. 1998 Uniaxial exchange flows of two Bingham fluids in a cylindrical duct. *IMA J. Appl. Maths* **61**, 237–266.

Frigaard, I. A. & Scherzer, O. 2000 The effects of yield stress variation on uniaxial exchange flows of two Bingham fluids in a pipe. *SIAM J. Appl. Maths* **60**, 1950–1976.

Gabard, C. 2001 Etude de la stabilité de films liquides sur les parois d'une conduite verticale lors de l'ecoulement de fluides miscibles non-Newtoniens. These de l'Universite Pierre et Marie Curie (PhD thesis), Orsay, France.

Gabard, C. & Hulin, J.-P. 2003 Miscible displacements of non-Newtonian fluids in a vertical tube. *Eur. Phys. J.* E **11**, 231–241.

Glowinski, R. 1984 *Numerical Methods for Nonlinear Variational Problems*. Springer.

Glowinski, R., Lions, J.-L. & Trémolières, R. 1981 *Numerical Analysis of Variational Inequalities*. North-Holland.

Hickox, C. E. 1971 Instability due to viscosity and density stratification in axisymmetric pipe flow. *Phys. Fluids* **14**, 251–262.

Hinch, E. J. 1984 A note on the mechanism of the instability at the interface between two shearing fluids. *J. Fluid Mech.* **114**, 463–465.

Hinch, E. J., Harris, O. J. & Rallison, J. M. 1992 The instability mechanism for two elastic fluids being co-extruded. *J. Non-Newtonian Fluid Mech.* **43**, 311–324.

Hooper, A. P. & Boyd, W. G. 1987 Shear flow instability due to a wall and a viscosity discontinuity at the interface. *J. Fluid Mech.* **179**, 201–225.

Hoppe, R. H. W., Mazurkevitch, G., Rettig, U. & von Stryk, O. 1999 *Modelling, Simulation and Control of Electrorheological Fluid Devices*. SFB-438-9917, preprint series, T.-U. München

Huilgol, R. R. & Pannizza, M. P. 1995 On determination of the plug flow region in Bingham fluids through the application of variational inequalities. *J. Non-Newtonian Fluid Mech.* **58**, 207–217.

Joseph, D. D. 1976 *Stability of Fluid Motions I*. Springer.

Joseph, D. D. & Carmi, S. 1969 Stability of Poiseuille flow in pipes, annuli, and channels. *Q. Appl. Maths* **26**, 575–599.

Joseph, D. D. & Renardy, Y. Y. 1993 *Fundamentals of Two-Fluid Dynamics*. Springer.

Khomami, B. 1990 Interfacial stability and deformation of two stratified power law fluids in plane Poiseuille flow, part 1. stability analysis. *J. Non-Newtonian Fluid Mech.* **36**, 289–303.

Larson, R. G. 1992 Instabilities in viscoelastic flows. *Rheol. Acta* **31**, 213–263.

Moyers-Gonzalez, M. A. 2002 Nonlinearly stable multi-layer visco-plastic fluids. MSc thesis, University of British Columbia, August 2002.

Moyers-Gonzalez, M. A. & Frigaard, I. A. 2003 Numerical solution of duct flows of multiple visco-plastic fluids. *J. Non-Newtonian Fluid Mech.* (accepted).

Nouar, C. & Frigaard, I. A. 2001 Nonlinear stability of Poiseuille flow of a Bingham fluid: theoretical results and comparison with phenomenological criteria. *J. Non-Newtonian Fluid Mech.* **100**, 127–149.

Pinarbasi, A. & Liakopoulos, A. 1995 Stability of two-layer Poiseuille flow of Carreau-Yasuda and Bingham-like fluids. *J. Non-Newtonian Fluid Mech.* **57**, 227–241.

Saramito, P. & Roquet, N. 2001 An adaptive finite element method for viscoplastic fluid flows in pipes. *Comput. Meth. Appl. Mech. Engng* **190**, 5391–5412.

Su, Y. Y. & Khomami, B. 1991 Stability of multi-layer power law and second order fluids in plane Poiseuille flow. *Chem. Engng Commun.* **109**, 209–223.

Vola, D., Boscardin, L. & Latché, J. C. 2003 Laminar unsteady flows of Bingham fluids: a numerical strategy and some benchmark results. *J. Comput. Phys.* **187**, 441–456.

Waters, N. D. 1983 The stability of two stratified power law fluids in Couette flow. *J. Non-Newtonian Fluid Mech.* **12**, 85–94.

Waters, N. D. & Keeley, A. M. 1987 The stability of two stratified non-Newtonian liquids in Couette flow. *J. Non-Newtonian Fluid Mech.* **24**, 161–181.

Yiantsos, S. G. & Higgins, B. G. 1988 Linear stability of plane Poiseuille flow of two superposed fluids. *Phys. Fluids* **31**, 3225–3238.

Yih, C.-S. 1967 Instability due to viscosity stratification. *J. Fluid Mech.* **27**, 337–352.